



TECH BRIEFS

NATIONAL AERONAUTICS AND SPACE ADMINISTRATION

-  **Technology Focus**
-  **Electronics/Computers**
-  **Software**
-  **Materials**
-  **Mechanics**
-  **Machinery/Automation**
-  **Manufacturing & Prototyping**
-  **Bio-Medical**
-  **Physical Sciences**
-  **Information Sciences**
-  **Books and Reports**

INTRODUCTION

Tech Briefs are short announcements of innovations originating from research and development activities of the National Aeronautics and Space Administration. They emphasize information considered likely to be transferable across industrial, regional, or disciplinary lines and are issued to encourage commercial application.

Availability of NASA Tech Briefs and TSPs

Requests for individual Tech Briefs or for Technical Support Packages (TSPs) announced herein should be addressed to

National Technology Transfer Center

Telephone No. (800) 678-6882 or via World Wide Web at www2.nttc.edu/leads/

Please reference the control numbers appearing at the end of each Tech Brief. Information on NASA's Innovative Partnerships Program (IPP), its documents, and services is also available at the same facility or on the World Wide Web at <http://ipp.nasa.gov>.

Innovative Partnerships Offices are located at NASA field centers to provide technology-transfer access to industrial users. Inquiries can be made by contacting NASA field centers listed below.

NASA Field Centers and Program Offices

Ames Research Center

Lisa L. Lockyer
(650) 604-1754
lisa.l.lockyer@nasa.gov

Dryden Flight Research Center

Gregory Poteat
(661) 276-3872
greg.poteat@dfrc.nasa.gov

Goddard Space Flight Center

Nona Cheeks
(301) 286-5810
nona.k.cheeks@nasa.gov

Jet Propulsion Laboratory

Ken Wolfenbarger
(818) 354-3821
james.k.wolfenbarger@jpl.nasa.gov

Johnson Space Center

Michele Brekke
(281) 483-4614
michele.a.brekke@nasa.gov

Kennedy Space Center

David R. Makufka
(321) 867-6227
david.r.makufka@nasa.gov

Langley Research Center

Martin Waszak
(757) 864-4052
martin.r.waszak@nasa.gov

Glenn Research Center

Robert Lawrence
(216) 433-2921
robert.f.lawrence@nasa.gov

Marshall Space Flight Center

Vernotto McMillan
(256) 544-2615
vernotto.mcmillan@msfc.nasa.gov

Stennis Space Center

John Bailey
(228) 688-1660
john.w.bailey@nasa.gov

Carl Ray, Program Executive

Small Business Innovation
Research (SBIR) & Small
Business Technology
Transfer (STTR) Programs
(202) 358-4652
carl.g.ray@nasa.gov

Merle McKenzie

Innovative Partnerships
Program Office
(202) 358-2560
merle.mckenzie-1@nasa.gov



TECH BRIEFS

NATIONAL AERONAUTICS AND SPACE ADMINISTRATION



5 Technology Focus: Sensors

- 5 Flexible Skins Containing Integrated Sensors and Circuitry
- 6 Artificial Hair Cells for Sensing Flows
- 7 Video Guidance Sensor and Time-of-Flight Rangefinder
- 8 Optical Beam-Shear Sensors



11 Electronics/Computers

- 11 Multiple-Agent Air/Ground Autonomous Exploration Systems
- 12 A 640 × 512-Pixel Portable Long-Wavelength Infrared Camera
- 13 An Array of Optical Receivers for Deep-Space Communications
- 14 Microstrip Antenna Arrays on Multilayer LCP Substrates
- 15 Applications for Subvocal Speech
- 15 Multiloop Rapid-Rise/Rapid Fall High-Voltage Power Supply



17 Software

- 17 The PICWidget
- 17 Fusing Symbolic and Numerical Diagnostic Computations
- 17 Probabilistic Reasoning for Robustness in Automated Planning
- 17 Short-Term Forecasting of Radiation Belt and Ring Current
- 18 JMS Proxy and C/C++ Client SDK
- 18 XML Flight/Ground Data Dictionary Management
- 18 Cross-Compiler for Modeling Space-Flight Systems



19 Materials

- 19 Composite Elastic Skins for Shape-Changing Structures
- 19 Glass/Ceramic Composites for Sealing Solid Oxide Fuel Cells



21 Mechanics

- 21 Aligning Optical Fibers by Means of Actuated MEMS Wedges



23 Manufacturing & Prototyping

- 23 Manufacturing Large Membrane Mirrors at Low Cost
- 23 Double-Vacuum-Bag Process for Making Resin-Matrix Composites



25 Bio-Medical

- 25 Surface Bacterial-Spore Assay Using Tb3+/DPA Luminescence
- 25 Simplified Microarray Technique for Identifying mRNA in Rare Samples



27 Physical Sciences

- 27 High-Resolution, Wide-Field-of-View Scanning Telescope
- 28 Multispectral Imager With Improved Filter Wheel and Optics
- 29 Integral Radiator and Storage Tank
- 30 Compensation for Phase Anisotropy of a Metal Reflector
- 31 Optical Characterization of Molecular Contaminant Films



33 Information Sciences

- 33 Integrated Hardware and Software for No-Loss Computing
- 33 Decision-Tree Formulation With Order-1 Lateral Execution



35 Books & Reports

- 35 GIS Methodology for Planning Planetary-Rover Operations
- 35 Optimal Calibration of the Spitzer Space Telescope
- 35 Automated Detection of Events of Scientific Interest
- 35 Representation-Independent Iteration of Sparse Data Arrays
- 36 Mission Operations of the Mars Exploration Rovers
- 36 More About Software for No-Loss Computing

This document was prepared under the sponsorship of the National Aeronautics and Space Administration. Neither the United States Government nor any person acting on behalf of the United States Government assumes any liability resulting from the use of the information contained in this document, or warrants that such use will be free from privately owned rights.



Technology Focus: Sensors

Flexible Skins Containing Integrated Sensors and Circuitry

Densely arrayed tactile sensors measure multiple, spatially registered physical quantities simultaneously.

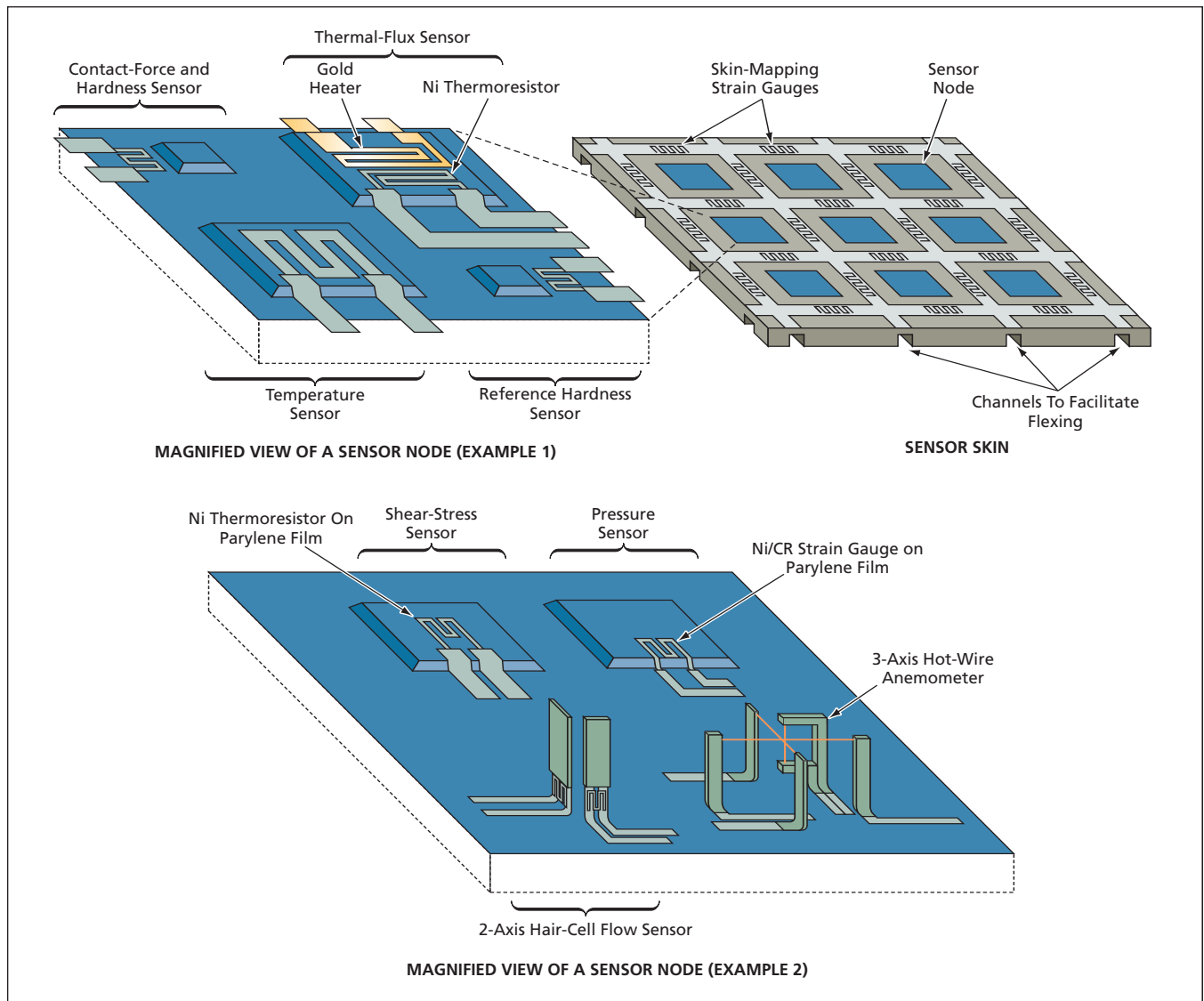
Goddard Space Flight Center, Greenbelt, Maryland

Artificial sensor skins modeled partly in imitation of biological sensor skins are undergoing development. These sensor skins comprise flexible polymer substrates that contain and/or support dense one- and two-dimensional arrays of microscopic sensors and associated microelectronic circuits. They afford multiple tactile sensing modalities for measuring physical phenomena that can

include contact forces; hardnesses, temperatures, and thermal conductivities of objects with which they are in contact; and pressures, shear stresses, and flow velocities in fluids. The sensor skins are mechanically robust, and, because of their flexibility, they can be readily attached to curved and possibly moving and flexing surfaces of robots, wind-tunnel models, and other objects that one

might seek to equip for tactile sensing.

Because of the diversity of actual and potential sensor-skin design criteria and designs and the complexity of the fabrication processes needed to realize the designs, it is not possible to describe the sensor-skin concept in detail within this article. Instead, an approximation of the concept is illustrated here by means of the following two examples:



A **Sensor Skin** contains an array of sensor nodes, each node containing multiple sensors that measure different quantities. The sensor nodes shown here are examples only: the variety of potential sensor-node designs is practically unlimited.

The top part of the figure depicts a skin containing a two-dimensional array of sensor nodes. Each sensor node contains (1) a temperature sensor; (2) a combination of force sensors that have different stiffnesses and that, in combination, provide information on both contact force and hardness; and (3) a thermal-flux sensor.

The gaps between the sensor nodes contain strain gauges, which serve as auxiliary sensors for measuring bending of the sensor skin: The strains measured by the strain gauges can be used to estimate the three-dimensional configuration of the skin and, hence, the three-dimensional location of each sensor node. In addition to enabling the assignment of sensory data to specific locations, this three-dimensional information can be useful for measuring and/or controlling the movement of an instrumented object.

A sensor skin like this one is typically fabricated on a 2-mil (≈ 0.05 -mm)-thick polyimide substrate, which affords a combination of flexibility, robustness,

and low material cost. Patterned thin metal films are used as piezoresistors, heaters, and temperature transducers, which serve as building blocks of sensors. The sensors and associated circuitry are formed by microfabrication techniques that do not involve high temperatures. Some of these techniques are adapted from fabrication of integrated circuits on rigid substrates, while others have been developed specifically for use on flexible polymeric substrates.

The bottom part of the figure depicts a multimodal sensor node that is one of many such nodes arrayed in a flow-sensing skin. The node contains (1) a pressure sensor comprising a strain gauge on a surface-micromachined parylene diaphragm, (2) a shear-stress sensor comprising a thermoresistor on another surface-micromachined parylene diaphragm, (3) a trio of surface-micromachined hot-wire anemometers for measuring flow velocity in three dimensions, and (4) a pair of surface-micromachined hair-cell sensors for measuring

flow velocity in two dimensions along the skin.

The hair-cell sensors are particularly noteworthy inasmuch as they implement an approximation of the same sensory principle as that of flow-sensing cilia of fish. A cilium is bent by an amount proportional to the flow to which it is exposed. In the artificial sensor skin, the bending of an artificial cilium is measured by means of a strain gauge at its base.

This work was done by Chang Liu of the University of Illinois at Urbana-Champaign for Goddard Space Flight Center.

In accordance with Public Law 96-517, the contractor has elected to retain title to this invention. Inquiries concerning rights for its commercial use should be addressed to:

*University of Illinois at Urbana-Champaign
319 Ceramics Bldg, MC-243
105 South Goodwin Avenue
Urbana, IL 61801*

Refer to GSC-14821-1, volume and number of this NASA Tech Briefs issue, and the page number.

Artificial Hair Cells for Sensing Flows

Small, robust sensors can be fabricated on a variety of substrates.

Goddard Space Flight Center, Greenbelt, Maryland

The purpose of this article is to present additional information about the flow-velocity sensors described briefly in the immediately preceding article. As noted therein, these sensors can be characterized as artificial hair cells that implement

an approximation of the sensory principle of flow-sensing cilia of fish: A cilium is bent by an amount proportional to the flow to which it is exposed. A nerve cell at the base of the cilium senses the flow by sensing the bending of the cilium. In

an artificial hair cell, the artificial cilium is a microscopic cantilever beam, and the bending of an artificial cilium is measured by means of a strain gauge at its base (see Figure 1).

Figure 2 presents cross sections of a representative sensor of this type at two different stages of its fabrication process. The process consists of relatively-low-temperature metallization, polymer-deposition, microfabrication, and surface-micromachining subprocesses, including plastic-deformation magnetic assembly (PDMA), which is described below. These subprocesses are suitable for a variety of substrate materials, including silicon, some glasses, and some polymers. Moreover, because it incorporates a polymeric supporting structure, this sensor is more robust, relative to its silicon-based counterparts. The fabrication process consists mainly of the following steps:

1. A $0.5\text{-}\mu\text{m}$ -thick sacrificial layer of Al is deposited (by evaporation) and patterned on a substrate.
2. A $5.8\text{-}\mu\text{m}$ -thick layer of a photodefinable polyimide is spun on and patterned photolithographically. The polyimide is



Figure 1. **Artificial-Hair-Cell Flow Sensors** shown in this scanning electron micrograph have several different widths as well as different heights ranging from 0.6 to 1.5 mm.

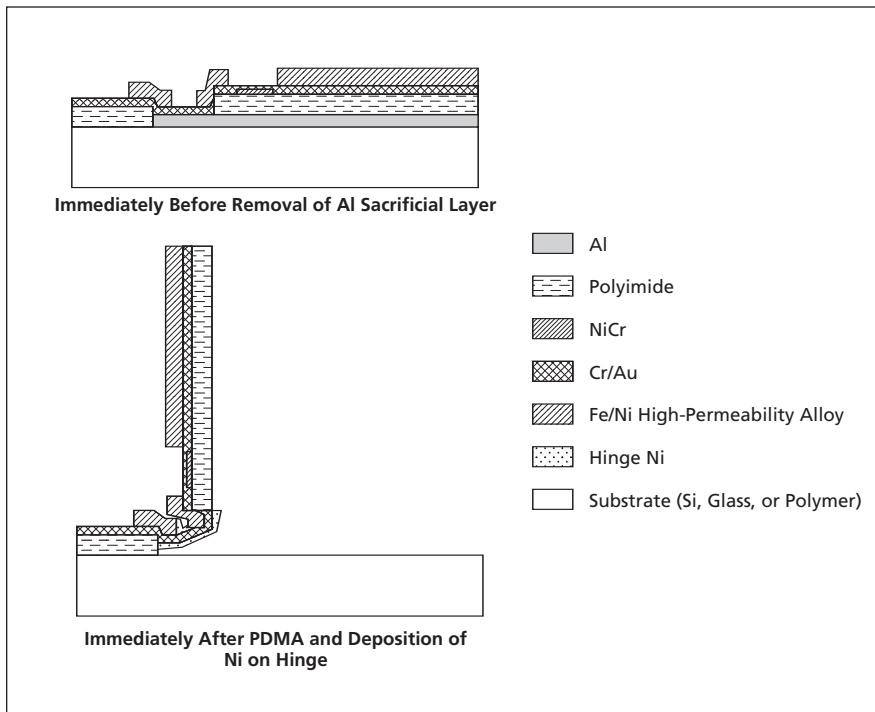


Figure 2. **The Cantilever Remains Horizontal** during most of the fabrication process. It is released by etching away the aluminum sacrificial layer, then raised to its perpendicular orientation by PDMA.

2. The workpiece is cured in a 1-torr (≈ 133 -Pa) atmosphere of N_2 for 2 hours at a temperature of $350^\circ C$ (this is the highest temperature used in the fabrication process).
3. A 750-\AA -thick layer of NiCr, intended to serve as the electrically resistive transducer in the strain gauge, is deposited by electron-beam evaporation.
4. A layer of Au/Cr $0.5\ \mu m$ thick, from which the strain-gauge electrical leads and a bending hinge are to be formed, is deposited by evaporation.
5. A portion of the Au/Cr layer also serves as a seed layer for electrodeposition of a $5\text{-}\mu m$ -thick layer of a highly magnetically permeable Fe/Ni alloy. Once this

alloy has been deposited, the remaining unused Au/Cr is removed by lift-off.

6. A $1.8\text{-}\mu m$ -thick polyimide film (omitted from the figure) is deposited to form a protective coat on the Fe/Ni alloy layer and the NiCr strain gauge.
7. The workpiece is placed in a basic solution for more than a day to etch away the sacrificial layer of Al.
8. The workpiece is rinsed, then placed in an electroplating bath. A magnetic field is applied to pull up on the Fe/Ni layer, thereby bending the cantilever upward at the hinge. While the magnetic field remains thus applied, Ni is electrodeposited onto the Au/Cr hinge to a thickness of $\approx 10\ \mu m$, thereby reinforcing the hinge and fixing the cantilever perpendicular to the substrate.

This work was done by Chang Liu and Jack Chen of the University of Illinois at Urbana-Champaign for Goddard Space Flight Center.

In accordance with Public Law 96-517, the contractor has elected to retain title to this invention. Inquiries concerning rights for its commercial use should be addressed to

*University of Illinois at Urbana-Champaign
Office of Technology Management
319 Ceramics Building, MC-243
105 South Goodwin Avenue
Urbana, IL 61801*

Refer to GSC-14812-1, volume and number of this NASA Tech Briefs issue, and the page number.

Video Guidance Sensor and Time-of-Flight Rangefinder

A prior VGS would be modified to incorporate the rangefinder function.

Marshall Space Flight Center, Alabama

A proposed video guidance sensor (VGS) would be based mostly on the hardware and software of a prior Advanced VGS (AVGS), with some additions to enable it to function as a time-of-flight rangefinder (in contradistinction to a triangulation or image-processing rangefinder). It would typically be used at distances of the order of 2 or 3 kilometers, where a typical target would appear in a video image as a single blob, making it possible to extract the direction to the target (but not the orientation of the target or the distance to the target) from a video image of light reflected from the target.

As described in several previous *NASA Tech Briefs* articles, an AVGS system is an optoelectronic system that provides guidance for automated docking of two

vehicles. In the original application, the two vehicles are spacecraft, but the basic principles of design and operation of the system are applicable to aircraft, robots, objects maneuvered by cranes, or other objects that may be required to be aligned and brought together automatically or under remote control. In a prior AVGS system of the type upon which the now-proposed VGS is largely based, the tracked vehicle is equipped with one or more passive targets that reflect light from one or more continuous-wave laser diode(s) on the tracking vehicle, a video camera on the tracking vehicle acquires images of the targets in the reflected laser light, the video images are digitized, and the image data are processed to obtain the direction to the target.

The design concept of the proposed VGS does not call for any memory or processor hardware beyond that already present in the prior AVGS, but does call for some additional hardware and some additional software. It also calls for assignment of some additional tasks to two subsystems that are parts of the prior VGS: a field-programmable gate array (FPGA) that generates timing and control signals, and a digital signal processor (DSP) that processes the digitized video images.

The additional timing and control signals generated by the FPGA would cause the VGS to alternate between an imaging (direction-finding) mode and a time-of-flight (range-finding mode) and would govern operation in the range-finding mode. In the direction-finding mode, the VGS would function as described

above. In the range-finding mode, the laser diode(s) would be toggled between two programmed power levels, while the intensities of the outgoing and return laser beams would be sensed by two matched photodetectors. The outputs of the photodetectors would be sent to dedicated high-speed analog-to-digital converters, the outputs of which would be stored (buffered) for processing.

The DSP would execute algorithms that would determine the time between corresponding transitions of the outgoing and return signals and, hence,

equivalently, the time of flight of the laser signal and the distance to the target. The algorithms would be modern ones that would enable determination of the time of flight to within a small fraction of the transition time between the two laser power levels, even if the outgoing and return laser waveforms were slow, nonlinear, or noisy. The DSP would also execute an algorithm that would determine the return signal level and would accordingly adjust the laser output and the gain of a programmable-gain amplifier.

This work was done by Thomas Bryan, Richard Howard, Joseph L. Bell, Fred D. Roe, and Michael L. Book of Marshall Space Flight Center. Further information is contained in a TSP (see page 1).

This invention has been patented by NASA (U.S. Patent No. 7,006,203). Inquiries concerning nonexclusive or exclusive license for its commercial development should be addressed to Sammy Nabors, MSFC Commercialization Assistance Lead, at sammy.a.nabors@nasa.gov. Refer to MFS-31785-1.

Optical Beam-Shear Sensors

Simple sensors measure radiant fluxes in beam quadrants.

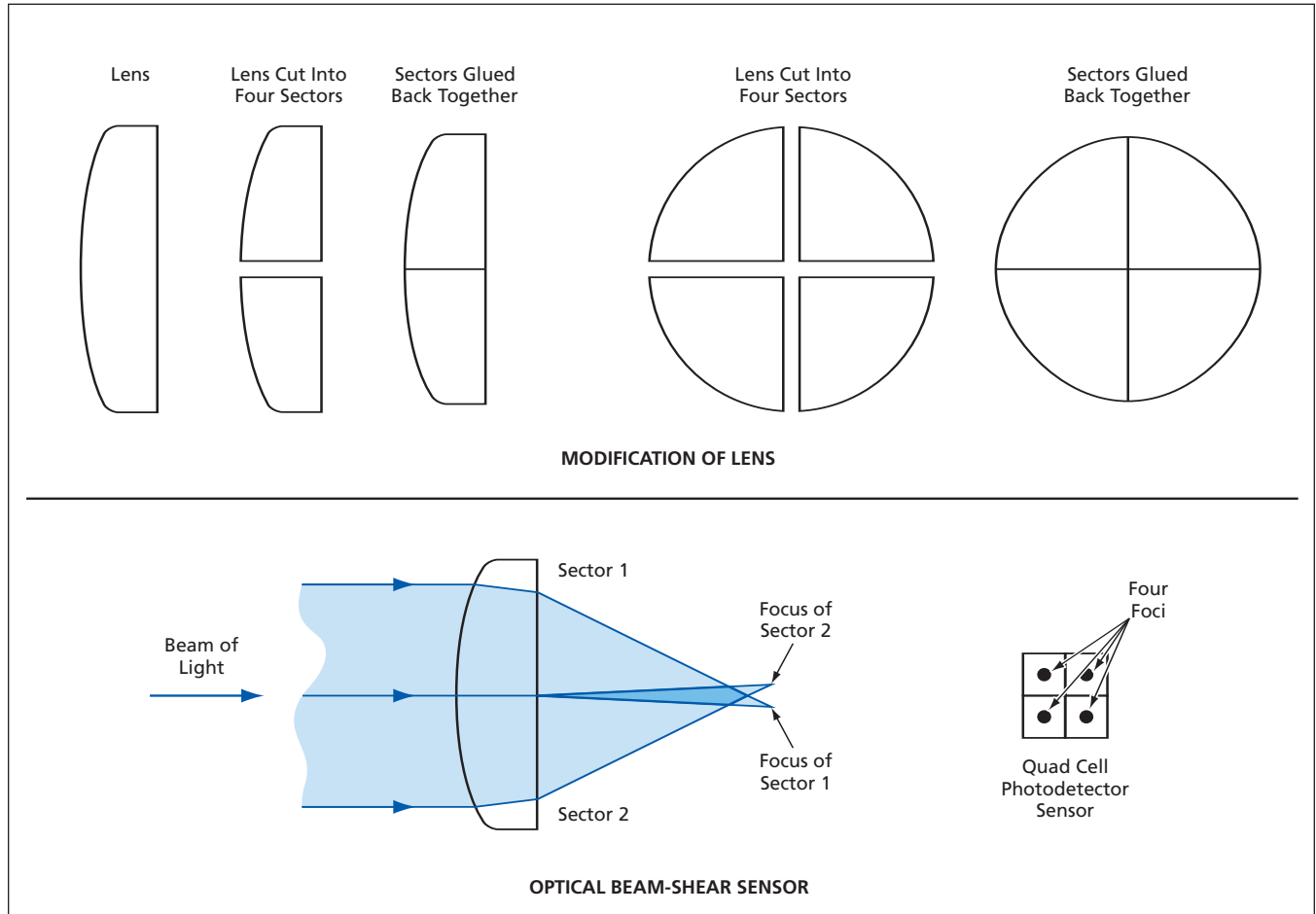
NASA's Jet Propulsion Laboratory, Pasadena, California

A technique for measuring optical beam shear is based on collecting light from the four quadrants of the beam and comparing the optical power collected from each quadrant with that from the other three quadrants. As

used here, "shear" signifies lateral displacement of a beam of light from a nominal optical axis.

A sensor for implementing this technique consists of a modified focusing lens and a quad-cell photodetector,

both centered on the nominal optical axis. The modification of the lens consists in cutting the lens into four sectors (corresponding to the four quadrants) by sawing along two orthogonal diameters, then reassembling the lens follow-



An Optical Beam-Shear Sensor can be made from a lens and a quad-cell photodetector.

ing either of two approaches described next.

In one approach, the lens is re-assembled by gluing the sectors back together. In the simplest variant of this approach, the kerf of the saw matches the spacing of the photodetector cells, so that the focus of each sector crosses the axis of symmetry to

fall on the opposite photodetector cell (see figure). In another variant of this approach, the lens sectors are spaced apart to make their individual foci to fall on separate photodetector cells, without crossing the optical axis. In the case of a sufficiently wide beam, the modified lens could be replaced with four independent lenses

placed in a square array, each focusing onto an independent photodetector.

*This work was done by Stefan Martin and Piotr Szwaykowski of Caltech for NASA's Jet Propulsion Laboratory. Further information is contained in a TSP (see page 1).
NPO-41746*



Multiple-Agent Air/Ground Autonomous Exploration Systems

These systems would cover large areas and would function robustly.

NASA's Jet Propulsion Laboratory, Pasadena, California

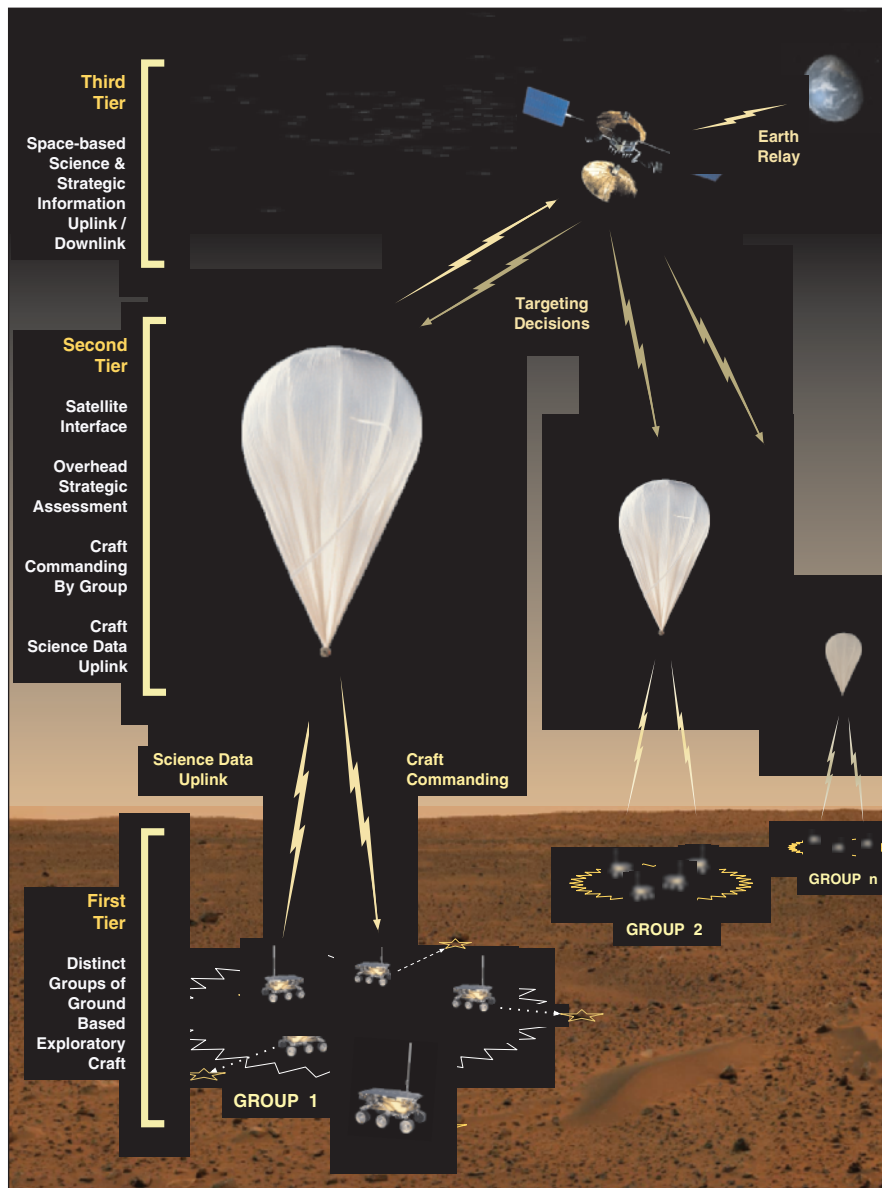
Autonomous systems of multiple-agent air/ground robotic units for exploration of the surfaces of remote planets are undergoing development. Modified versions of these systems could be used on Earth to perform tasks in environments dangerous or inaccessible to humans: examples of tasks could include scientific exploration of remote

regions of Antarctica, removal of land mines, cleanup of hazardous chemicals, and military reconnaissance.

A basic system according to this concept (see figure) would include a unit, suspended by a balloon or a blimp, that would be in radio communication with multiple robotic ground vehicles (rovers) equipped with video cameras

and possibly other sensors for scientific exploration. The airborne unit would be free-floating, controlled by thrusters, or tethered either to one of the rovers or to a stationary object in or on the ground. Each rover would contain a semiautonomous control system for maneuvering and would function under the supervision of a control system in the airborne unit. The rover maneuvering control system would utilize imagery from the onboard camera to navigate around obstacles. Avoidance of obstacles would also be aided by readout from an onboard (e.g., ultrasonic) sensor. Together, the rover and airborne control systems would constitute an overarching closed-loop control system to coordinate scientific exploration by the rovers.

The rovers would be relatively inexpensive (and, hence, somewhat expendable) units equipped with task-specific sensors. The redundancy afforded by the use of many such rovers (in contradistinction to a single, more generally capable and thus more expensive rover) would help to ensure the success in the event of loss of one or a few rovers. The use of many rovers would also make it possible to cover a large terrain area in a short time. The airborne unit would have an overhead perspective that would enable it to provide guidance to the rovers. For example, the airborne unit could "see" a scientifically interesting terrain feature or a hazard or obstacle hidden from a rover camera by an intervening hill. One or more camera(s) in the airborne unit would acquire terrain images that would be digitized and processed by feature-extraction algorithms. The feature data would be used by planning algorithms to choose potential targets for close examination by the rovers and for planning the paths of the rovers across the terrain. The paths would be chosen to enable the rovers to avoid obstacles and hazards (e.g., hills and cliffs) on their way to their designated targets. Among the planning algorithms would be algorithms for prioritization and sequencing of targets. There would also be algorithms for re-



A Balloon-Borne Unit would supervise the maneuvers of multiple rovers from an overhead perspective.

planning in response to information on local conditions observed by the rovers and in response to deviations of rovers from planned paths.

Once a rover reached a target, it would acquire close-up images and possibly other sensory information about the target. Features would be extracted from the image data and from any other sensory data to characterize the site. Then the rover would be commanded to move on to the next target. The exploratory process as described thus far would be repeated by each rover until all targets in the terrain area of interest had been examined. A partly functional model of such a system operates in a 4-by-5-ft (1.22-

by-1.52-m) test bed that simulates terrain.

The test bed is strewn with variously colored and shaped blocks to simulate targets and obstacles. An overhead view is provided by a camera on a mast above the center of the test bed. Miniature rovers equipped with cameras maneuver on the simulated terrain. At the time of reporting the information for this article, efforts to develop a more fully functional model for testing advanced hardware and software designs were under way.

This work was done by Wolfgang Fink, Tien-Hsin Chao, Jay Hanan, and Mark Tarbell of Caltech, and James M. Dohm of the University of Arizona for NASA's Jet Propulsion Laboratory. Further informa-

tion is contained in a TSP (see page 1).

In accordance with Public Law 96-517, the contractor has elected to retain title to this invention. Inquiries concerning rights for its commercial use should be addressed to:

*Innovative Technology Assets Management
JPL*

Mail Stop 202-233

4800 Oak Grove Drive

Pasadena, CA 91109-8099

(818) 354-2240

E-mail: iaoffice@jpl.nasa.gov

Refer to NPO-40428, volume and number of this NASA Tech Briefs issue, and the page number.

A 640 × 512-Pixel Portable Long-Wavelength Infrared Camera

This hand-held camera shows promise for imaging at high thermal resolution.

NASA's Jet Propulsion Laboratory, Pasadena, California

A portable long-wavelength infrared electronic camera having a cutoff wavelength of 9 μm has been built around an image sensor in the form of a 640 × 512-pixel array of $\text{Al}_x\text{Ga}_{1-x}\text{As}/\text{GaAs}$ quantum-well infrared photodetectors (QWIPs). This camera is an intermediate product of a continuing program to develop high-resolution, high-sensitivity infrared cameras.

Major features of the design and fabrication of the camera are the following:

- The QWIPs are of the bound-to-quasi-bound type, for which the thermionic component of dark current is less than for other types. [This concept was discussed in more detail in "Bound-to-Quasi-Bound Quantum-Well Infrared Photodetectors" (NPO-19633), *NASA Tech Briefs*, Vol. 22, No. 9 (September 1998), page 54.]
- The basic multiple-quantum-well (MQW) structure of the QWIP array in the present camera is a stack of about 50 identical quantum-well bilayers. Each bilayer comprises (1) a 45-Å-thick well layer of GaAs n-doped at a density $\approx 5 \times 10^{17} \text{ cm}^{-3}$ and (2) a 500-Å-thick barrier layer of $\text{Al}_{0.3}\text{Ga}_{0.7}\text{As}$.
- The MQW structure is sandwiched between 0.5- μm -thick top and bottom contact layers of GaAs doped similarly to the well layers.
- All of the aforementioned layers were fabricated on a semi-insulating GaAs substrate by molecular-beam epitaxy. A 300-Å-thick $\text{Al}_{0.3}\text{Ga}_{0.7}\text{As}$ stop-etch layer was grown on top of the top contact layer. A 0.7- μm -thick GaAs cap layer



This Image Was Generated From One Frame of video readout, at frame rate of 30 Hz, from the camera described in the text.

was grown on top of the stop-etch layer. A cross-grating structure for coupling light into the QWIPs was fabricated in the cap layer by photolithography and dry chemical etching. [The cross-grating-coupler concept was described in "Cross-Grating Coupling for Focal-Plane Arrays of QWIPs" (NPO-19657), *NASA Tech Briefs*, Vol. 22, No. 1 (January 1998), page 6a.]

- The array of 640 × 512 photodetectors, with a pitch of 25 μm and a pixel size of 23 × 23 μm^2 , was then formed by wet chemical etching through the MQW

layers into the bottom contact layer. The cross gratings on the tops of the detectors thus formed were covered with Au/Ge and Au for ohmic contact and reflection.

- Indium bumps were evaporated onto the top (Au/Ge)/Au layers, then the bumps were used to bond (hybridize) the array to a silicon-based complementary metal oxide semiconductor (CMOS) integrated-circuit 640 × 512 readout multiplexer.

As described thus far, with the exception of the sizes and numbers of pixels,

the QWIP-array/readout-multiplexer is nearly identical to that of the prior camera. An important difference is that in the present camera, the readout multiplexer is part of a commercial infrared-camera body that includes two “back-end” video-signal-processing circuits and a germanium lens of 100-mm focal length and 5.5° field of view. The lens is designed to be transparent in the wavelength range of 7 to 14 μm (compatible with a nominal QWIP operational wavelength of 8.5 μm). The digital acquisition resolution of the camera circuitry is 14 bits, so that the instantaneous dynamic range of the cam-

era is 16,384. However, the dynamic range of the QWIPs is 85 dB.

The camera has been demonstrated to produce excellent video imagery (see figure). Whereas prior infrared cameras based on detectors of different types have been limited to thermal resolutions in excess of 30 mK, this camera is expected to exhibit significantly finer thermal resolution: On the basis of single-pixel test data, a noise equivalent differential temperature of 8 mK is expected in operation at a temperature of 65 K with $f/2$ (focal length \div aperture diameter = 2) optics and a background temperature of 300 K. The

array of photodetectors has exhibited background-limited performance at an operating temperature of 72 K using the same optics and background conditions. Optimization of operating conditions (including frame rate, integration time, and QWIP bias voltage) is expected to lead to even better performance.

This work was done by Sarath Gunapala, Sumith Bandara, John Liu, and Sir B. Rafol of Caltech for NASA's Jet Propulsion Laboratory. Further information is contained in a TSP (see page 1). NPO-30624

An Array of Optical Receivers for Deep-Space Communications

This array would be considerably simpler and less expensive to implement.

NASA's Jet Propulsion Laboratory, Pasadena, California

An array of small optical receivers is proposed as an alternative to a single large optical receiver for high-data-rate communications in NASA's Deep Space Network (DSN). Because the telescope for a single receiver capable of satisfying DSN requirements must be greater than 10 m in diameter, the design, building, and testing of the telescope would be very difficult and expensive. The proposed array would utilize commercially available telescopes of 1-m or smaller diameter and, therefore, could be developed and verified with considerably less difficulty and expense.

The essential difference between a single-aperture optical-communications receiver and an optical-array receiver is that a single-aperture receiver focuses all of the light energy it collects onto the surface of an optical detector, whereas an array receiver focuses portions of the total collected energy onto separate detectors, optically detects each fractional energy component, then combines the electrical signal from the array of detector outputs to form the observable, or “decision statistic,” used to decode the transmitted data.

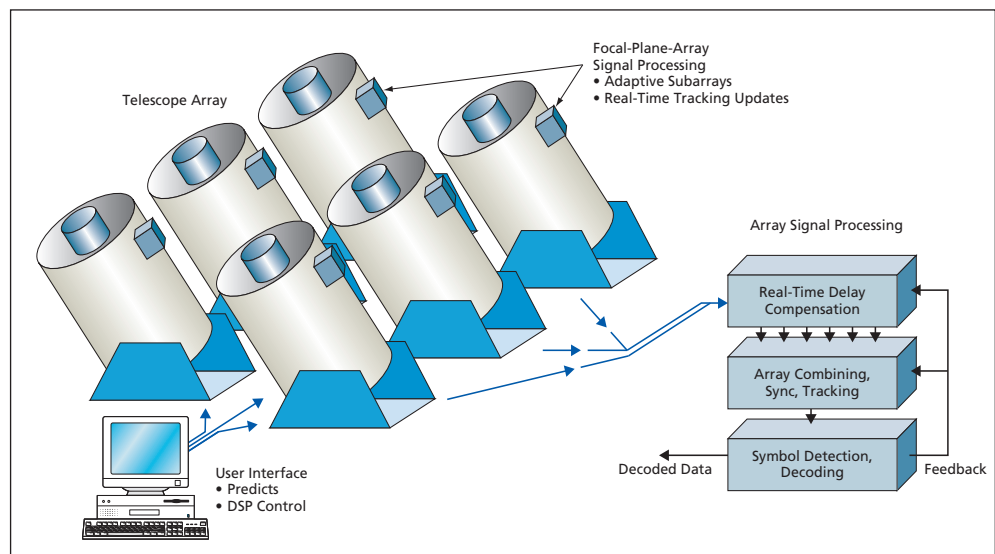
A conceptual block diagram identifying the key components of the optical-array receiver suitable for deep-space telemetry reception is shown in the figure. The most conspicuous feature of the receiver is the large number of small- to medium-size telescopes, with individual apertures and

number of telescopes selected to make up the desired total collecting area. This array of telescopes is envisioned to be fully computer-controlled via the user interface and prediction-driven to achieve rough pointing and tracking of the desired spacecraft. Fine-pointing and tracking functions then take over to keep each telescope pointed toward the source, despite imperfect pointing predictions, telescope-drive errors, and vibration caused by wind.

The turbulence-degraded image of the laser source in each telescope would be sensed by a focal-plane photodetector array, the outputs of which would then be digitized. The digitized array outputs would be synchronized and combined by field-programmable gate-

array circuits that would execute digital-signal-processing algorithms, for both the individual telescopes and the entire array. Symbol detection and decoding operations would then be carried out on the synchronized and combined array signal. Receiver parameters would be controlled adaptively at each telescope to accommodate changing atmospheric conditions, thus optimizing the performance of the optical-array receiver in real time.

This work was done by Victor Vilnrotter, Chi-Wung Lau, Meera Srinivasan, Kenneth Andrews, and Ryan Mukai of Caltech for NASA's Jet Propulsion Laboratory. Further information is contained in a TSP (see page 1). NPO-40190



A Conceptual Block Diagram of the Optical-Array Receiver identifies key receiver functions.

Microstrip Antenna Arrays on Multilayer LCP Substrates

Antennas, feedlines, and switches are embedded in and on flexible sheets.

John H. Glenn Research Center, Cleveland, Ohio

A research and development effort now underway is directed toward satisfying requirements for a new type of relatively inexpensive, lightweight, microwave antenna array and associated circuitry packaged in a thin, flexible sheet that can readily be mounted on a curved or flat rigid or semi-rigid surface. A representative package of this type consists of microwave antenna circuitry embedded in and/or on a multilayer liquid-crystal polymer (LCP) substrate. The

circuitry typically includes an array of printed metal microstrip patch antenna elements and their feedlines on one or more of the LCP layer(s). The circuitry can also include such components as electrostatically actuated microelectromechanical systems (MEMS) switches for connecting and disconnecting antenna elements and feedlines. In addition, the circuitry can include switchable phase shifters described below.

LCPs were chosen over other flexible

substrate materials because they have properties that are especially attractive for high-performance microwave applications. These properties include low permittivity, low loss tangent, low water-absorption coefficient, and low cost. By means of heat treatments, their coefficients of thermal expansion can be tailored to make them more amenable to integration into packages that include other materials. The nature of the flexibility of LCPs is such that large LCP sheets containing antenna arrays can be rolled up, then later easily unrolled and deployed.

Figure 1 depicts a prototype three-LCP-layer package containing two four-element, dual-polarization microstrip-patch arrays: one for a frequency of 14 GHz, the other for a frequency of 35 GHz. The 35-GHz patches are embedded on top surface of the middle [15-mil (≈ 0.13 -mm)-thick] LCP layer; the 14-GHz patches are placed on the top surface of the upper [9-mil (≈ 0.23 -mm)-thick] LCP layer. The particular choice of LCP layer thicknesses was made on the basis of extensive analysis of the effects of the thicknesses on cross-polarization levels, bandwidth, and efficiency at each frequency.

The diagonal orientation of the microstrip patches in Figure 1 is not inherent in the LCP implementation: instead, it is part of an example design for a typical intended application in radar measurement of precipitation, in which there would be a requirement that both the 14- and the 35-GHz arrays exhibit

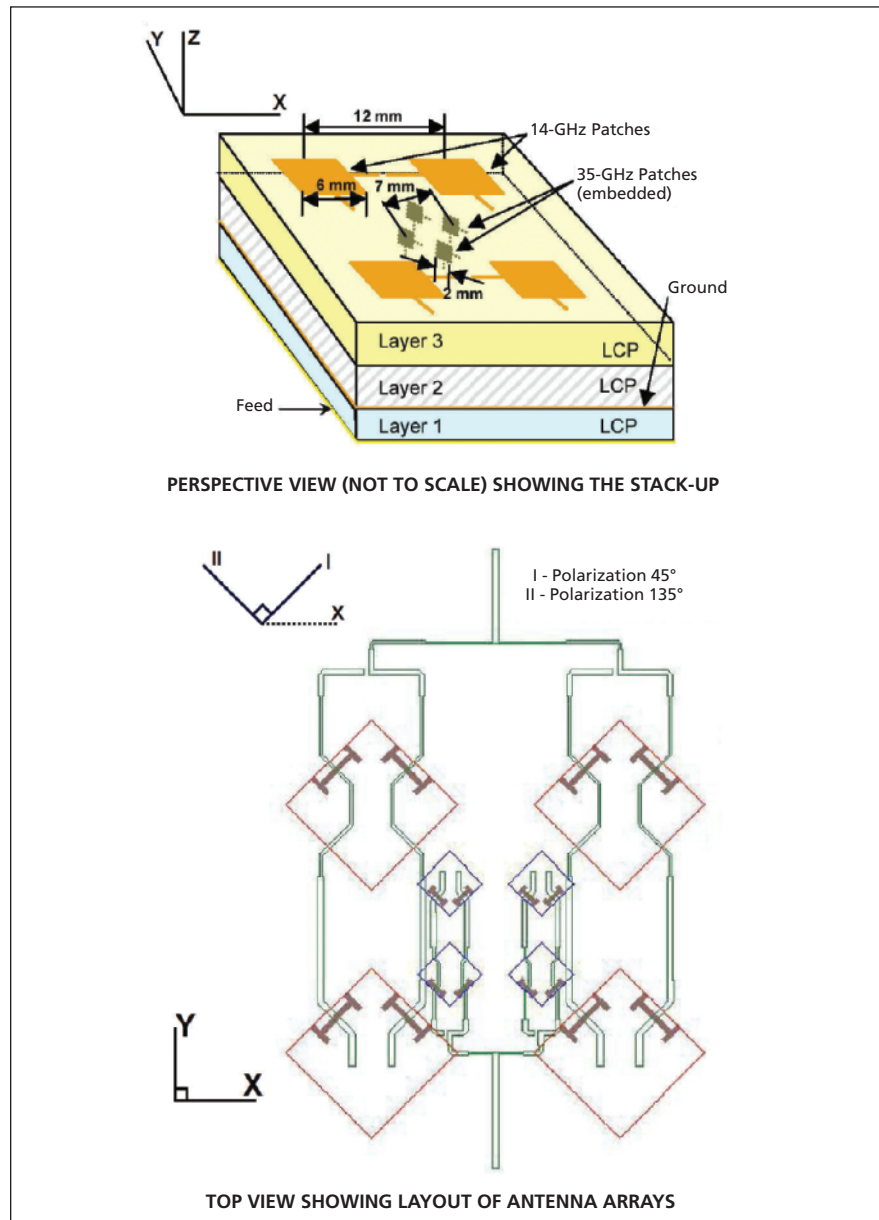


Figure 1. A Dual-Frequency, Dual-Polarization Array of microstrip patch antenna elements is packaged with three layers of LCP.

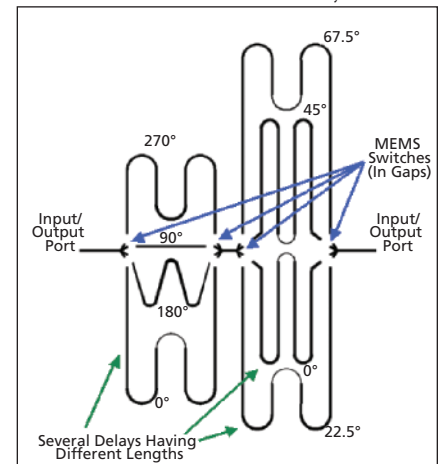


Figure 2. MEMS Switches are used to connect the input/output ports to one of the two delay lines to obtain one or the other of two different amounts of phase shift.

similar orthogonal-polarization characteristics, including high degrees of polarization purity. The diagonal orientation helps in realizing a symmetrical feed network for both polarizations with similar impedance characteristics and radiation patterns. RF MEMS switches would be included in a production model but are not included in the prototype: Instead, to simplify computational simulation and testing, switching of polarizations is represented by the presence of hard-wired open and short circuits at switch locations.

Figure 2 is a plan view of a switchable phase shifter — in this case, one that can be switched between two different phase shifts. The device includes electrostatically actuated RF MEMS switches that

are used to make and break connections to eight microstrip delay lines having different lengths (e.g., 1 wavelength versus $3/4$ wavelength). Necessarily omitting details for the sake of brevity, each MEMS switch includes a microscopic flexible electrically conductive member that, through application of a suitably large DC bias voltage, can be pulled into proximity with microstrip conductors on opposite sides of the gap. The flexible member is covered to prevent direct electrical contact with the microstrip conductors, but the effect of the proximity is such as to enable substantial capacitive coupling of the microwave signal across the gap. The measured loss of the four-bit packaged phase shifter is only 0.24 dB per bit with a phase error less

than 4° at 14 GHz. At the time of this reporting, this is the first package flexible organic RF MEMS multibit phase shifter ever documented.

This work was done by Dane Thompson, Ramanan Bairavasubramanian, Guoan Wang, Nickolas D. Kingsley, Ioannis Pappolymerou, Emmanouil M. Tenteris, Gerald DeJean, and RongLin Li of Georgia Institute of Technology for Glenn Research Center. Further information is contained in a TSP (see page 1).

Inquiries concerning rights for the commercial use of this invention should be addressed to NASA Glenn Research Center, Innovative Partnerships Office, Attn: Steve Fedor, Mail Stop 4-8, 21000 Brookpark Road, Cleveland, Ohio 44135. Refer to LEW-17980-1.

Applications for Subvocal Speech

Ames Research Center, Moffett Field, California

A research and development effort now underway is directed toward the use of subvocal speech for communication in settings in which (1) acoustic noise could interfere excessively with ordinary vocal communication and/or (2) acoustic silence or secrecy of communication is required. By “subvocal speech” is meant sub-audible electromyographic (EMG) signals, associated with speech, that are acquired from the surface of the larynx and lingual areas of the throat. Topics addressed in this effort include recogni-

tion of the sub-vocal EMG signals that represent specific original words or phrases; transformation (including encoding and/or enciphering) of the signals into forms that are less vulnerable to distortion, degradation, and/or interception; and reconstruction of the original words or phrases at the receiving end of a communication link. Potential applications include ordinary verbal communications among hazardous-material-cleanup workers in protective suits, workers in noisy environments, divers, and firefighters, and

secret communications among law-enforcement officers and military personnel in combat and other confrontational situations.

This work was done by Charles Jorgensen of Ames Research Center and Bradley Betts of Computer Sciences Corporation.

This invention is owned by NASA and a patent application has been filed. Inquiries concerning rights for the commercial use of this invention should be addressed to the Ames Technology Partnerships Division at (650) 604-2954. Refer to ARC-15519-1.

Multiloop Rapid-Rise/Rapid Fall High-Voltage Power Supply

Marshall Space Flight Center, Alabama

A proposed multiloop power supply would generate a potential as high as 1.25 kV with rise and fall times $<100 \mu\text{s}$. This power supply would, moreover, be programmable to generate output potentials from 20 to 1,250 V and would be capable of supplying a current of at least 300 μA at 1,250 V. This power supply is intended to be a means of electronic shuttering of a microchannel plate that would be used to intensify the output of a charge-coupled-device imager to obtain exposure times as short as 1 ms. The basic design of this power supply could also be adapted to other applications in which high voltages and high slew rates are needed. At the time of reporting the information for this

article, there was no commercially available power supply capable of satisfying the stated combination of voltage, rise-time, and fall-time requirements.

The power supply would include a preregulator that would be used to program a voltage $1/30$ of the desired output voltage. By means of a circuit that would include a pulse-width modulator (PWM), two voltage doublers, and a transformer having two primary and two secondary windings, the preregulator output voltage would be amplified by a factor of 30. A resistor would limit the current by controlling a drive voltage applied to field-effect transistors (FETs) during turn-on of the PWM. Two feed-

back loops would be used to regulate the high output voltage. A pulse transformer would be used to turn on four FETs to short-circuit output capacitors when the outputs of the PWM were disabled. Application of a 0-to-5-V square to a PWM shut-down pin would cause a 20-to-1,250-V square wave to appear at the output.

This work was done by Douglas Bearden of Marshall Space Flight Center.

This invention is owned by NASA, and a patent application has been filed. For further information, contact Sammy Nabors, MSFC Commercialization Assistance Lead, at sammy.a.nabors@nasa.gov. Refer to MFS-32137-1.



▶ The PICWidget

The Plug-in Image Component Widget (PICWidget) is a software component for building digital imaging applications. The component is part of a methodology described in “GIS Methodology for Planning Planetary-Rover Operations” (NPO-41812), which appears elsewhere in this issue of *NASA Tech Briefs*. Planetary rover missions return a large number and wide variety of image data products that vary in complexity in many ways. Supported by a powerful, flexible image-data-processing pipeline, the PICWidget can process and render many types of imagery, including (but not limited to) thumbnail, subframed, downsampled, stereoscopic, and mosaic images; images coregistered with orbital data; and synthetic red/green/blue images. The PICWidget is capable of efficiently rendering images from data representing many more pixels than are available at a computer workstation where the images are to be displayed. The PICWidget is implemented as an Eclipse plug-in using the Standard Widget Toolkit, which provides a straightforward interface for re-use of the PICWidget in any number of application programs built upon the Eclipse application framework. Because the PICWidget is tile-based and performs aggressive tile caching, it has flexibility to perform faster or slower, depending whether more or less memory is available.

This work was done by Jeffrey Norris, Jason Fox, Kenneth Rabe, I-Hsiang Shu, and Mark Powell of Caltech for NASA’s Jet Propulsion Laboratory. Further information is contained in a TSP (see page 1). This software is available for commercial licensing. Please contact Karina Edmonds of the California Institute of Technology at (626) 395-2322. Refer to NPO-41813.

▶ Fusing Symbolic and Numerical Diagnostic Computations

“X-2000 Anomaly Detection Language” denotes a developmental computing language, and the software that establishes and utilizes the language, for fusing two diagnostic computer programs, one implementing a numerical analysis method, the other implementing a symbolic analysis method into a unified event-based decision analysis software system for real-

time detection of events (e.g., failures) in a spacecraft, aircraft, or other complex engineering system. The numerical analysis method is performed by beacon-based exception analysis for multi-missions (BEAMs), which has been discussed in several previous *NASA Tech Briefs* articles. The symbolic analysis method is, more specifically, an artificial-intelligence method of the knowledge-based, inference engine type, and its implementation is exemplified by the Spacecraft Health Inference Engine (SHINE) software. The goal in developing the capability to fuse numerical and symbolic diagnostic components is to increase the depth of analysis beyond that previously attainable, thereby increasing the degree of confidence in the computed results. In practical terms, the sought improvement is to enable detection of all or most events, with no or few false alarms.

This program was written by Mark James of Caltech for NASA’s Jet Propulsion Laboratory. Further information is contained in a TSP (see page 1).

This software is available for commercial licensing. Please contact Karina Edmonds of the California Institute of Technology at (626) 395-2322. Refer to NPO-42512.

▶ Probabilistic Reasoning for Robustness in Automated Planning

A general-purpose computer program for planning the actions of a spacecraft or other complex system has been augmented by incorporating a subprogram that reasons about uncertainties in such continuous variables as times taken to perform tasks and amounts of resources to be consumed. This subprogram computes parametric probability distributions for time and resource variables on the basis of user-supplied models of actions and resources that they consume. The current system accepts bounded Gaussian distributions over action duration and resource use. The distributions are then combined during planning to determine the net probability distribution of each resource at any time point. In addition to a full combinatoric approach, several approximations for arriving at these combined distributions are available, including maximum-likelihood and pessimistic algorithms. Each

such probability distribution can then be integrated to obtain a probability that execution of the plan under consideration would violate any constraints on the resource. The key idea is to use these probabilities of conflict to score potential plans and drive a search toward planning low-risk actions. An output plan provides a balance between the user’s specified averseness to risk and other measures of optimality.

This program was written by Steven Schaffer, Bradley Clement, and Steve Chien of Caltech for NASA’s Jet Propulsion Laboratory. Further information is contained in a TSP (see page 1).

This software is available for commercial licensing. Please contact Karina Edmonds of the California Institute of Technology at (626) 395-2322. Refer to NPO-42152.

▶ Short-Term Forecasting of Radiation Belt and Ring Current

A computer program implements a mathematical model of the radiation-belt and ring-current plasmas resulting from interactions between the solar wind and the Earth’s magnetic field, for the purpose of predicting fluxes of energetic electrons (10 keV to 5 MeV) and protons (10 keV to 1 MeV), which are hazardous to humans and spacecraft. Given solar-wind and interplanetary-magnetic-field data as inputs, the program solves the convection-diffusion equations of plasma distribution functions in the range of 2 to 10 Earth radii. Phenomena represented in the model include particle drifts resulting from the gradient and curvature of the magnetic field; electric fields associated with the rotation of the Earth, convection, and temporal variation of the magnetic field; and losses along particle-drift paths. The model can readily accommodate new magnetic- and electric-field submodels and new information regarding physical processes that drive the radiation-belt and ring-current plasmas. Despite the complexity of the model, the program can be run in real time on ordinary computers. At present, the program can calculate present electron and proton fluxes; after further development, it should be able to predict the fluxes 24 hours in advance.

This program was written by George V. Khazanov of Marshall Space Flight Center and Mei-Ching Fok of Goddard Space Flight Center. Further information is contained in a TSP (see page 1).MFS-32128-1

➤ JMS Proxy and C/C++ Client SDK

JMS Proxy and C/C++ Client SDK (“JMS” signifies “Java messaging service” and “SDK” signifies “software development kit”) is a software package for developing interfaces that enable legacy programs (here denoted “clients”) written in the C and C++ languages to communicate with each other via a JMS broker. This package consists of two main components: the JMS proxy server component and the client C library SDK component. The JMS proxy server component implements a native Java process that receives and responds to requests from clients. This component can run on any computer that supports Java and a JMS client. The client C library SDK component is used to develop a JMS client program running in each affected C or C++ environment, without need for running a Java virtual machine in the affected computer. A C client program developed by use of this SDK has most of the quality-of-service characteristics of standard Java-based client programs, including the following:

- Durable subscriptions;
- Asynchronous message receipt;
- Such standard JMS message qualities as “TimeToLive,” “Message Properties,” and “DeliveryMode” (as the quoted terms are defined in previously published JMS documentation); and
- Automatic reconnection of a JMS proxy to a restarted JMS broker.

This program was written by Paul Wolgast and Paul Pechkam of Caltech for NASA’s Jet Propulsion Laboratory. Further information is contained in a TSP (see page 1).

This software is available for commercial licensing. Please contact Karina Edmonds of the California Institute of Technology at (626) 395-2322. Refer to NPO-42527.

➤ XML Flight/Ground Data Dictionary Management

A computer program generates Extensible Markup Language (XML) files that effect coupling between the command- and telemetry-handling software running aboard a spacecraft and the corresponding software running in ground support systems. The XML files are produced by use of information from the flight software and from flight-system engineering. The XML files are converted to legacy ground-system data formats for command and telemetry, transformed into Web-based and printed documentation, and used in developing new ground-system data-handling software. Previously, the information about telemetry and command was scattered in various paper documents that were not synchronized. The process of searching and reading the documents was time-consuming and introduced errors. In contrast, the XML files contain all of the information in one place. XML structures can evolve in such a manner as to enable the addition, to the XML files, of the metadata necessary to track the changes and the associated documentation. The use of this software has reduced the extent of manual operations in developing a ground data system, thereby saving considerable time and removing errors that previously arose in the translation and transcription of software information from the flight to the ground system.

This program was written by Jesse Wright and Colette Wiklow of Caltech for NASA’s Jet Propulsion Laboratory. Further information is contained in a TSP (see page 1).

This software is available for commercial licensing. Please contact Karina Edmonds of the California Institute of Technology at (626) 395-2322. Refer to NPO-42291.

➤ Cross-Compiler for Modeling Space-Flight Systems

Ripples is a computer program that makes it possible to specify arbitrarily complex space-flight systems in an easy-to-learn, high-level programming language and to have the specification automatically translated into LibSim, which is a text-based computing language in which such simulations are implemented. LibSim is a very powerful simulation language, but learning it takes considerable time, and it requires that models of systems and their components be described at a very low level of abstraction. To construct a model in LibSim, it is necessary to go through a time-consuming process that includes modeling each subsystem, including defining its fault-injection states, input and output conditions, and the topology of its connections to other subsystems. Ripples makes it possible to describe the same models at a much higher level of abstraction, thereby enabling the user to build models faster and with fewer errors. Ripples can be executed in a variety of computers and operating systems, and can be supplied in either source code or binary form. It must be run in conjunction with a Lisp compiler.

This program was written by Mark James of Caltech for NASA’s Jet Propulsion Laboratory. Further information is contained in a TSP (see page 1).

This software is available for commercial licensing. Please contact Karina Edmonds of the California Institute of Technology at (626) 395-2322. Refer to NPO-42532.



Composite Elastic Skins for Shape-Changing Structures

Anisotropic stiffness properties can be tailored for specific applications.

Langley Research Center, Hampton, Virginia

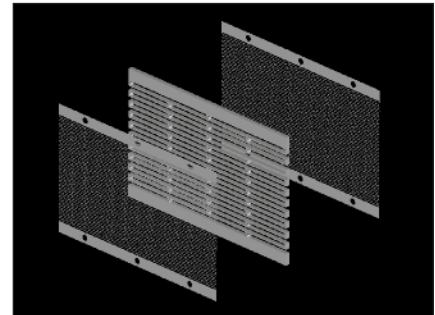
Composite elastic skins having tailorable mechanical properties have been invented for covering shape-changing (“morphable”) structures. These skins are intended especially for use on advanced aircraft that change shapes in order to assume different aerodynamic properties.

Many of the proposals for aircraft that could perform large aerodynamic shape changes require flexible skins that could follow shape changes of internal structures driven by actuators. Examples of such shape changes can include growth or shrinkage of bumps, conformal changes in wing planforms, cambers, twists, and bending of integrated leading- and trailing-edge flaps. Prior to this invention, there was no way of providing smooth aerodynamic surfaces capable of large deflections while maintaining smoothness and sufficient rigidity. Although latex rubber, silicone rubber, and similar conventional materials can be made into smooth coverings, they are not suitable for this purpose because, in order to impart required stiffness against out-of-plane bending, it would be necessary to make the coverings excessively thick, thereby necessitating the use of impractically large actuation forces.

The basic idea of the invention is that of smoothly wrapping an underlying variable structure with a smooth skin that

can be stretched or otherwise warped with low actuation force in one or both in-plane direction(s) and is relatively stiff against out-of-plane bending. It is envisioned that a skin according to the invention could be stretched as much as 20 percent in a desired direction. Because this basic idea admits of numerous variations, the following description is necessarily oversimplified for the sake of brevity.

A skin according to the invention can include one or more internal skeletal layer(s) made of a metal or a suitably stiff composite. By use of water-jet cutting, laser cutting, photolithography, or some other suitable technique, regular patterns of holes are cut into the skeletal layers (see figure). The skeletal layers are thereby made into planar springs. The skeletal layers are embedded in a castable elastomer. The anisotropic stiffness of the skin can be tailored through choice of the materials, the thicknesses of the skeletal and elastomeric layers, and the sizes and shapes of the cutouts. Moreover, by introducing local variations of thicknesses and/or cutout geometry, one can obtain local variations in the anisotropic stiffness. Threaded fasteners for attachment to actuators and/or the underlying structure are inserted in the internal skeleton at required locations.



Metal Skeletal Layers Are Patterned to obtain desired properties — in this case, to make them easily stretchable in the vertical direction but not in the horizontal direction. To complete the fabrication of a composite skin according to the invention, these metal skeletal layers would be embedded in an elastomeric sheet.

In one example typical of an important class of potential applications, the internal skeleton would be made less stiff in one in-plane direction. Such a skeleton would be desirable in an application in which the skin would be part of a hinge-like structure like a flap. In another example, the internal skeleton would be equally stiff in both in-plane directions, as would be desirable in application involving a planform change or a bump.

This work was done by Christopher M. Cagle and Robin W. Schlecht of Langley Research Center. Further information is contained in a TSP (see page 1). LAR-16599-1

Glass/Ceramic Composites for Sealing Solid Oxide Fuel Cells

Ceramic fillers in a glass contribute to strength and fracture toughness.

John H. Glenn Research Center, Cleveland, Ohio

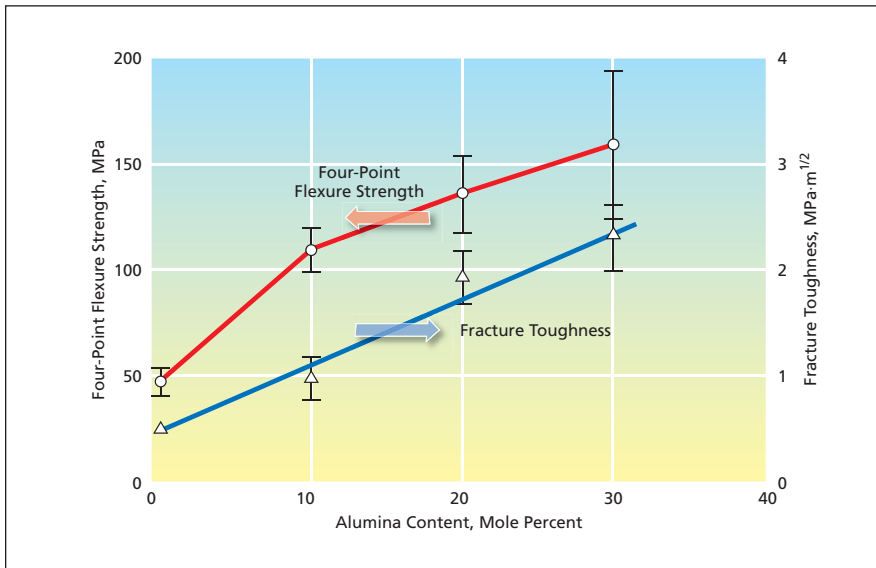
A family of glass/ceramic composite materials has been investigated for use as sealants in planar solid oxide fuel cells. These materials are modified versions of a barium calcium aluminosilicate glass developed previously for the same purpose. The composition of the glass in mole percentages is $35\text{BaO} + 15\text{CaO} + 5\text{Al}_2\text{O}_3 + 10\text{B}_2\text{O}_3 + 35\text{SiO}_2$. The glass seal was found to be susceptible to cracking during ther-

mal cycling of the fuel cells.

The goal in formulating the glass/ceramic composite materials was to (1) retain the physical and chemical advantages that led to the prior selection of the barium calcium aluminosilicate glass as the sealant while (2) increasing strength and fracture toughness so as to reduce the tendency toward cracking. Each of the composite formulations consists of the glass plus either

of two ceramic reinforcements in a proportion between 0 and 30 mole percent. One of the ceramic reinforcements consists of alumina platelets; the other one consists of particles of yttria-stabilized zirconia wherein the yttria content is 3 mole percent (3YSZ).

In preparation for experiments, panels of the glass/ceramic composites were hot-pressed and machined into test bars.



Four-Point Flexure Strength and Fracture Toughness were found to increase by factors of 2.3 and 3.5, respectively, with incorporation of 30 mole percent of alumina platelets.

Properties of the test bars, including four-point flexure strength, fracture toughness, modulus of elasticity, and density were determined. Four-point flexure strength and fracture toughness were found to increase with alumina or 3YSZ content (see figure). For the same mole percentage of ceramic, the increases in strength and fracture toughness were greater in the composites containing alumina than in the composites containing 3YSZ.

This work was done by Narottam P. Bansal of Glenn Research Center and Sung R. Choi of the University of Toledo. Further information is contained in a TSP (see page 1).

Inquiries concerning rights for the commercial use of this invention should be addressed to NASA Glenn Research Center, Innovative Partnerships Office, Attn: Steve Fedor, Mail Stop 4-8, 21000 Brookpark Road, Cleveland, Ohio 44135. Refer to LEW-17905-1.



Aligning Optical Fibers by Means of Actuated MEMS Wedges

Wedges would be fabricated using gray-scale exposure of photoresist.

Goddard Space Flight Center, Greenbelt, Maryland

Microelectromechanical systems (MEMS) of a proposed type would be designed and fabricated to effect lateral and vertical alignment of optical fibers with respect to optical, electro-optical, opto-electronic, and/or photonic devices on integrated circuit chips and similar monolithic device structures. A MEMS device of this type would consist of a pair of oppositely sloped alignment wedges attached to linear actuators that would translate the wedges in the plane of a substrate, causing an optical fiber in contact with the sloping wedge surfaces to undergo various displacements parallel and perpendicular to the plane. In making it possible to accurately align optical fibers individually during the packaging stages of fabrication of the affected devices, this MEMS device would also make it possible to relax tolerances in other stages of fabrication, thereby potentially reducing costs and increasing yields.

In a typical system according to the proposal (see Figure 1), one or more pair(s) of alignment wedges would be positioned to create a V groove in which an optical fiber would rest. The fiber would be clamped at a suitable distance from the wedges to create a cantilever with a slight bend to push the free end of the fiber gently to the bottom of the V groove. The wedges would be translated in the substrate plane by amounts Δx_1 and Δx_2 , respectively, which would be chosen to move the fiber parallel to the plane by a desired amount Δx and perpendicular to the plane by a desired amount Δy . The actuators used to translate the wedges could be variants of electrostatic or thermal actuators that are common in MEMS.

The wedges would be fabricated in batch processes by a method, already established in the art of MEMS, that involves gray-scale exposure of photoresist

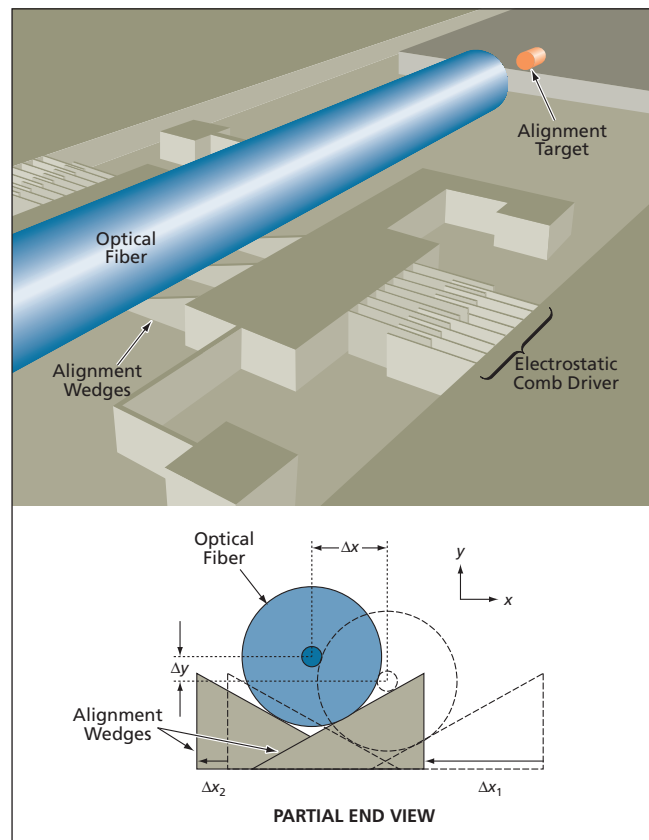


Figure 1. The Optical Fiber Would Be Displaced Vertically as Well as Horizontally in response to horizontal (only) displacements of the alignment wedges.

to create arbitrarily sloped features. To make such a wedge, one would begin by designing and fabricating an optical mask for use in partially exposing a photoresist film on a substrate of silicon or other suitable material. After a development step, each photoresist mask would have a desired shape — in this case, a wedge shape characterized by a variable height proportional to that of the desired final wedge shape (see Figure 2). Next, the workpiece would be subjected to a suitable dry plasma etching process (e.g., reactive-ion etching); what would remain after etching would be a wedge of substrate material having the desired slope.

In this gray-scale-based approach, subtle changes could be made in fabrication processes to tailor the angles and linear dimensions of the wedges in order to tailor the displace-

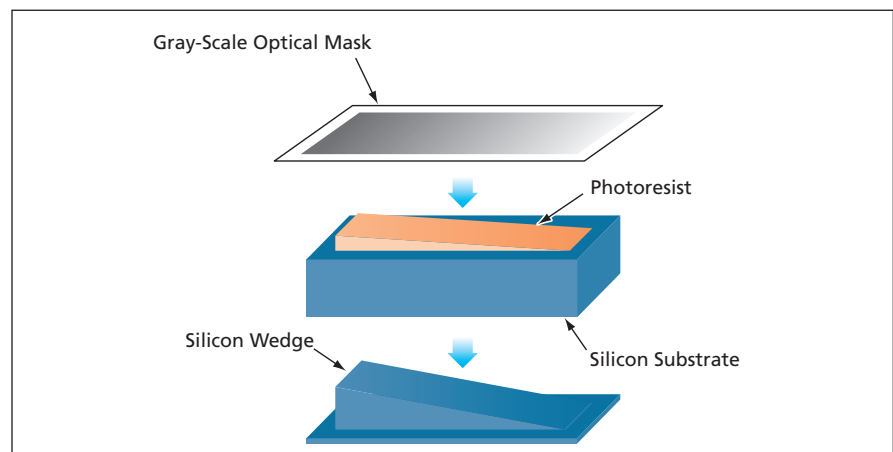


Figure 2. A Gray-Scale Optical Mask would be used to create a wedge of photoresist. Upon etching, a corresponding wedge shape would be imparted to the remaining silicon.

ment characteristics. This gray-scale approach could also be exploited to modify actuator characteristics by, for example, altering suspension geometries or profiles of capacitive surfaces.

*This work was done by Brian Morgan and Reza Ghodssi of the University of Maryland as part of a joint activity among the U.S. Army Research Laboratory, the Laboratory for Physical Sciences, and **Goddard Space***

Flight Center. For further information, contact the Goddard Innovative Partnerships Office at (301) 286-5810.
GSC-14959-1



Manufacturing Large Membrane Mirrors at Low Cost

Shapes are determined by edge retention fixtures rather than by precise molds.

Marshall Space Flight Center, Alabama

Relatively inexpensive processes have been developed for manufacturing lightweight, wide-aperture mirrors that consist mainly of reflectively coated, edge-supported polyimide membranes. The polyimide and other materials in these mirrors can withstand the environment of outer space, and the mirrors have other characteristics that make them attractive for use on Earth as well as in outer space:

- With respect to the smoothness of their surfaces and the accuracy with which they retain their shapes, these mirrors approach the optical quality of heavier, more expensive conventional mirrors.
- Unlike conventional mirrors, these mirrors can be stowed compactly and later deployed to their full sizes. In typical cases, deployment would be ef-

fectured by inflation.

Potential terrestrial and outer-space applications for these mirrors include large astronomical telescopes, solar concentrators for generating electric power and thermal power, and microwave reflectors for communication, radar, and short-distance transmission of electric power.

The relatively low cost of manufacturing these mirrors stems, in part, from the use of inexpensive tooling. Unlike in the manufacture of conventional mirrors, there is no need for mandrels or molds that have highly precise surface figures and highly polished surfaces. The surface smoothness is an inherent property of a polyimide film. The shaped area of the film is never placed

in contact with a mold or mandrel surface: Instead the shape of a mirror is determined by a combination of (1) the shape of a fixture that holds the film around its edge and (2) control of manufacturing-process parameters.

In a demonstration of this manufacturing concept, spherical mirrors having aperture diameters of 0.5 and 1.0 m were fabricated from polyimide films having thicknesses ranging from <20 μm to 150 μm . These mirrors have been found to maintain their preformed shapes following deployment.

This work was done by Larry J. Bradford of United Applied Technologies for Marshall Space Flight Center. Further information is contained in a TSP (see page 1). MFS-32176-1

Double-Vacuum-Bag Process for Making Resin-Matrix Composites

To prevent formation of voids, volatiles are removed before applying consolidation pressure.

Langley Research Center, Hampton, Virginia

A double-vacuum-bag process has been devised as a superior alternative to a single-vacuum-bag process used heretofore in making laminated fiber-reinforced resin-matrix composite-material structural components. This process is applicable to broad classes of high-performance matrix resins — including polyimides and phenolics — that emit volatile compounds (solvents and volatile by-products of resin-curing chemical reactions) during processing. The superiority of the double-vacuum-bag process lies in enhanced management of the volatile compounds. Proper management of volatiles is necessary for making composite-material components of high quality: if not removed and otherwise properly managed, volatiles can accumulate in interior pockets as resins cure, thereby forming undesired voids in the finished products.

The curing cycle for manufacturing a composite laminate containing a reactive resin matrix usually consists of a

two-step ramp-and-hold temperature profile and an associated single-step pressure profile as shown in Figure 1. The lower-temperature ramp-and-hold step is known in the art as the B stage. During the B stage, prepregs are heated and volatiles are generated. Because pressure is not applied at this stage, volatiles are free to escape. Pressure is applied during the higher-temperature ramp-and-hold step to consolidate the laminate and impart desired physical properties to the resin matrix. The residual volatile content and fluidity of the resin at the beginning of application of consolidation pressure are determined by the temperature and time parameters of the B stage. Once the consolidation pressure is applied, residual volatiles are locked in. In order to produce a void-free, high-quality laminate, it is necessary to design the curing cycle to obtain the required residual fluidity and the required temperature at the time of ap-

plication of the consolidation pressure.

Single-vacuum-bag processing in an oven is one of the most cost-effective techniques for making fiber-reinforced resin matrix composites in cases in which resins undergoing curing do not emit volatiles. However, this technique is often ineffective in cases in which volatiles are emitted. In order to produce a void-free composite laminate, it is imperative to remove the volatiles before commencing forced consolidation. A single-vacuum-bag assembly inherently hinders the removal of volatiles because the vacuum-induced compaction interferes with the vacuum-induced outgassing. The present double-vacuum-bag process eliminates this interference while still providing for vacuum-induced compaction.

Figure 2 depicts the double-vacuum-bag assembly used in this process. Fiber-reinforced, reactive-resin-matrix prepregs are laid up between a steel caul plate and a steel tool plate. This sub-

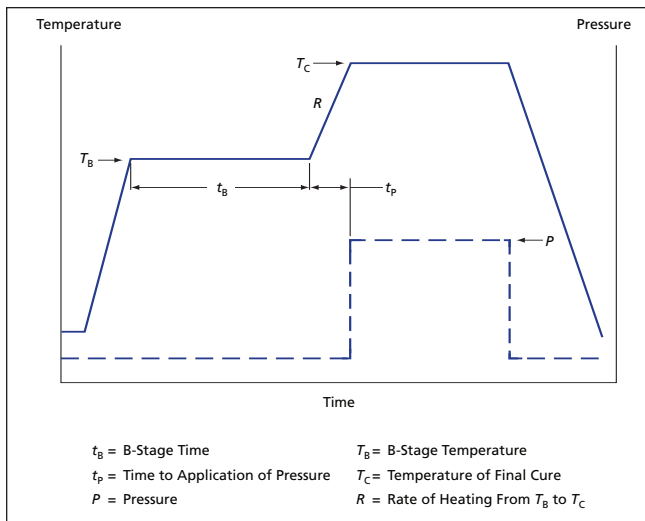


Figure 1. These **Temperature and Pressure Profiles** are typical of the curing cycle of a composite laminate containing a reactive resin matrix.

assembly is then enclosed by a vacuum bag, designated the inner bag, which is sealed around its edges onto the tool plate. Through a port built into the tool plate, the interior of the inner bag is connected to a vacuum pump. A tool that amounts to a perforated inverted bowl is placed on the tool plate outside the perimeter of the inner bag. Another vacuum bag, denoted the outer bag, is installed over the perforated inverted bowl, sealed to the tool plate, and connected to a vacuum pump in the same manner as that of the inner bag. The perforated inverted bowl must be rigid enough to withstand atmospheric pressure when the outer bag is evacuated.

This double-vacuum-bag assembly is

and subjected to prescribed curing cycle. During the B stage, full vacuum is applied in the outer bag, causing the outer bag to collapse onto the perforated inverted bowl. At the same time, a slightly lower vacuum [typically, a pressure of 2 in. Hg (≈ 7 kPa)] is applied in the inner bag. Because of the greater pressure in the inner bag, the inner bag expands against the perforated inverted bowl, leaving no compaction force on the composite layup. Hence, volatiles are free to escape and are removed by the inner-bag vacuum pump.

At the end of the B stage, the atmosphere is admitted to the interior of the outer bag, and full vacuum is applied in the inner bag. Therefore, the outer bag becomes loose from the perforated in-

verted bowl and the inner bag collapses onto the caul plate at atmospheric pressure, which now serves as the compaction pressure. The vacuum in the inner bag, and thus the compaction pressure, is maintained during the high-temperature ramp-and-hold period of the curing cycle.

This work was done by Tan-Hung Hou and Brian J. Jensen of Langley Research Center. Further information is contained in a TSP (see page 1).

This invention is owned by NASA, and a patent application has been filed. Inquiries concerning nonexclusive or exclusive license for its commercial development should be addressed to the Patent Counsel, Langley Research Center, at (757) 864-3521. Refer to LAR-16877.

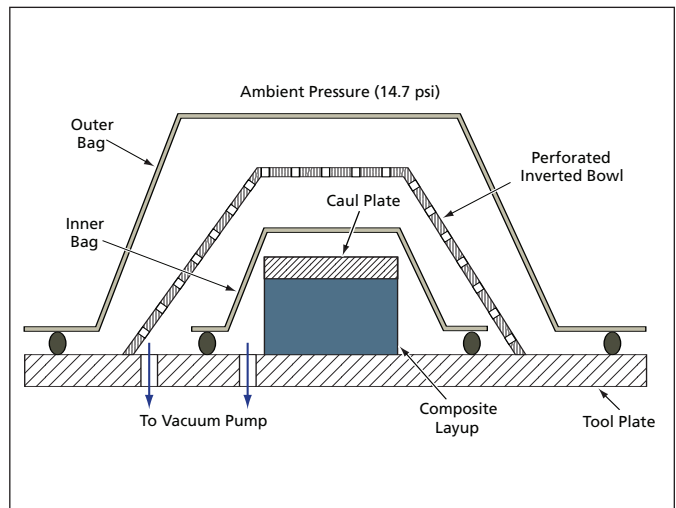


Figure 2. This **Double-Vacuum-Bag Assembly** makes it possible to maintain vacuum (for removal of volatiles) during the B stage, and then to apply consolidation pressure during the high-temperature curing stage.



Surface Bacterial-Spore Assay Using Tb^{3+} /DPA Luminescence

A total spore count could be obtained in minutes.

NASA's Jet Propulsion Laboratory, Pasadena, California

Equipment and a method for rapidly assaying solid surfaces for contamination by bacterial spores are undergoing development. The method would yield a total (non-viable plus viable) spore count of a surface within minutes and a viable-spore count in about one hour. In this method, spores would be collected from a surface by use of a transparent polymeric tape coated on one side with a polymeric adhesive that would be permeated with one or more reagent(s) for detection of spores by use of visible luminescence. The sticky side of the tape would be pressed against a surface to be assayed, then the tape with captured spores would be placed in a reader that illuminates the sample with ultraviolet light and counts the green luminescence spots under a microscope to quantify the number of bacterial spores per unit area. The visible luminescence spots seen through the microscope would be counted to determine the concentration of spores on the surface.

This method is based on the chemical and physical principles of methods described in several prior *NASA Tech Briefs* articles, including "Live/Dead Spore Assay Using DPA-Triggered Tb Luminescence" (NPO-30444), Vol. 27, No. 3 (March 2003), page 7a. To recapitulate: The basic idea is to exploit the observations that (1) dipicolinic

acid (DPA) is present naturally only in bacterial spores; and (2) when bound to Tb^{3+} ions, DPA triggers intense green luminescence of the ions under ultraviolet excitation; (3) DPA can be released from the viable spores by using L-alanine to make them germinate; and (4) by autoclaving, microwaving, or sonicating the sample, one can cause all the spores (non-viable as well as viable) to release their DPA.

One candidate material for use as the adhesive in the present method is polydimethylsiloxane (PDMS). In one variant of the method — for obtaining counts of all (viable and nonviable) spores — the PDMS would be doped with $TbCl_3$. After collection of a sample, the spores immobilized on the sticky tape surface would be lysed by heating or microwaving to release their DPA. Tb^{3+} ions from the $TbCl_3$ would become bound to the released DPA. The tape would then be irradiated with ultraviolet and examined as described above. In another variant of the method — for obtaining counts of viable spores only — the PDMS would be doped with L-alanine in addition to $TbCl_3$.

As now envisioned, a fully developed apparatus for implementing this method would include a pulsed source of ultraviolet light and a time-gated electronic camera to record the images seen

through the microscope during a prescribed exposure interval at a prescribed short time after an ultraviolet pulse. As in the method of the second-mentioned prior article, the pulsing and time-gating would be used to discriminate between the longer-lived Tb^{3+} /DPA luminescence and the shorter-lived background luminescence in the same wavelength range. In a time-gated image, the bright luminescence from bacterial spores could easily be seen against a dark background.

This work was done by Adrian Ponce of Caltech for NASA's Jet Propulsion Laboratory. Further information is contained in a TSP (see page 1).

In accordance with Public Law 96-517, the contractor has elected to retain title to this invention. Inquiries concerning rights for its commercial use should be addressed to:

*Innovative Technology Assets Management
JPL*

*Mail Stop 202-233
4800 Oak Grove Drive
Pasadena, CA 91109-8099
(818) 354-2240*

E-mail: iaoffice@jpl.nasa.gov

Refer to NPO-40646, volume and number of this NASA Tech Briefs issue, and the page number.

Simplified Microarray Technique for Identifying mRNA in Rare Samples

This method can be implemented by use of portable equipment.

Ames Research Center, Moffett Field, California

Two simplified methods of identifying messenger ribonucleic acid (mRNA), and compact, low-power apparatuses to implement the methods, are at the proof-of-concept stage of development. These methods are related to traditional methods based on hybridization of nucleic acid, but whereas the traditional methods must be practiced in laboratory settings, these methods could be practiced in field settings.

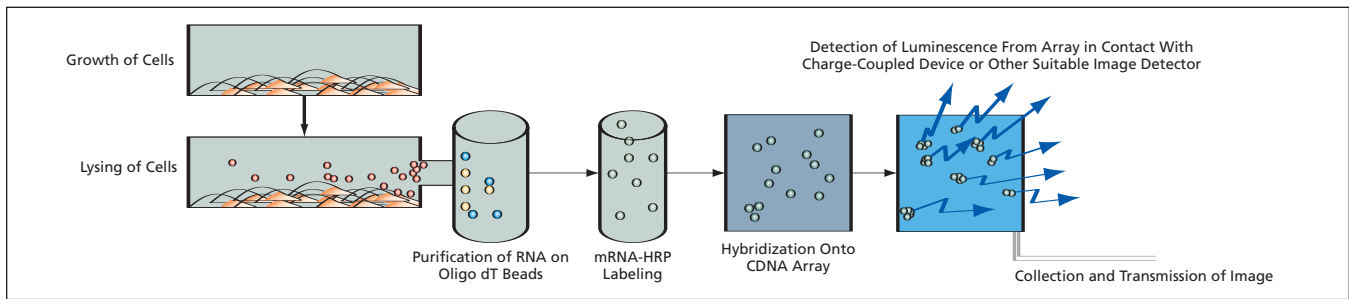
Hybridization of nucleic acid is a

powerful technique for detection of specific complementary nucleic acid sequences, and is increasingly being used for detection of changes in gene expression in microarrays containing thousands of gene probes. A traditional microarray study entails at least the following six steps:

1. Purification of cellular RNA,
2. Amplification of complementary deoxyribonucleic acid [cDNA] by poly-

- merase chain reaction (PCR),
3. Labeling of cDNA with fluorophores of Cy3 (a green cyanine dye) and Cy5 (a red cyanine dye),
4. Hybridization to a microarray chip,
5. Fluorescence scanning the array(s) with dual excitation wavelengths, and
6. Analysis of the resulting images.

This six-step procedure must be performed in a laboratory because it requires bulky equipment.



mRNA Is Labeled with a reporter enzyme (HRP), then hybridized onto a cDNA array. The array is then treated to induce chemiluminescence, which is detected by contact digital imaging.

The present developmental methods require fewer steps and are not restricted to laboratory settings because they do not require bulky equipment. In principle, they could be implemented by means of low-power, portable, lightweight units having sizes of the order of a cubic foot ($\approx 0.03\text{m}^3$). These methods could be used to perform field studies as precursors to full laboratory gene-expression analyses and can be used for detecting rare and little-expressed mRNA samples. This present method does not require the PCR-amplification, fluorescent-labeling, and scanning steps (steps 2, 3, and 5 listed above).

The steps involved in the method are depicted schematically in the figure. In this method, the initial mRNA from cell or tissue lysates is purified in one step, using oligo dT beads, and is then directly labeled by cross-linking to a reporter enzyme [horseradish peroxidase (HRP)]. The HRP-linked mRNA is then hybridized to a cDNA gene array printed on a nylon membrane, the membrane is incubated with a chemiluminescence substrate, and the resulting chemiluminescence from the affected area of the membrane is detected by contact digital imaging. The whole procedure takes less than five hours. This method is useful for identifying rare genes without much

processing, and for diagnostic genomic screening for biomarkers. The apparatus for implementing this method can be miniaturized for rapid screening for stem-cell research or analyzing rare cell samples from tissues.

This work was done by Eduardo Almeida of Ames Research Center and Geeta Kadambi of National Space Grant Foundation. Further information is contained in a TSP (see page 1).

This invention is owned by NASA and a patent application has been filed. Inquiries concerning rights for the commercial use of this invention should be addressed to the Ames Technology Partnerships Division at (650) 604-2954. Refer to ARC-15177-1.



High-Resolution, Wide-Field-of-View Scanning Telescope

Narrow-angle scanning over a wide field would be achieved without slewing the entire telescope.

NASA's Jet Propulsion Laboratory, Pasadena, California

A proposed telescope would afford high resolution over a narrow field of view ($<0.10^\circ$) while scanning over a total field of view nominally 16° wide without need to slew the entire massive telescope structure. The telescope design enables resolution of a 1-m-wide object in a 50-km-wide area of the surface of the Earth as part of a 200-km-wide area field of view monitored from an orbit at an altitude of 700 km. The conceptual design of this telescope could also be adapted to other applications — both terrestrial and extraterrestrial — in which there are requirements for telescopes that afford both wide- and narrow-field capabilities.

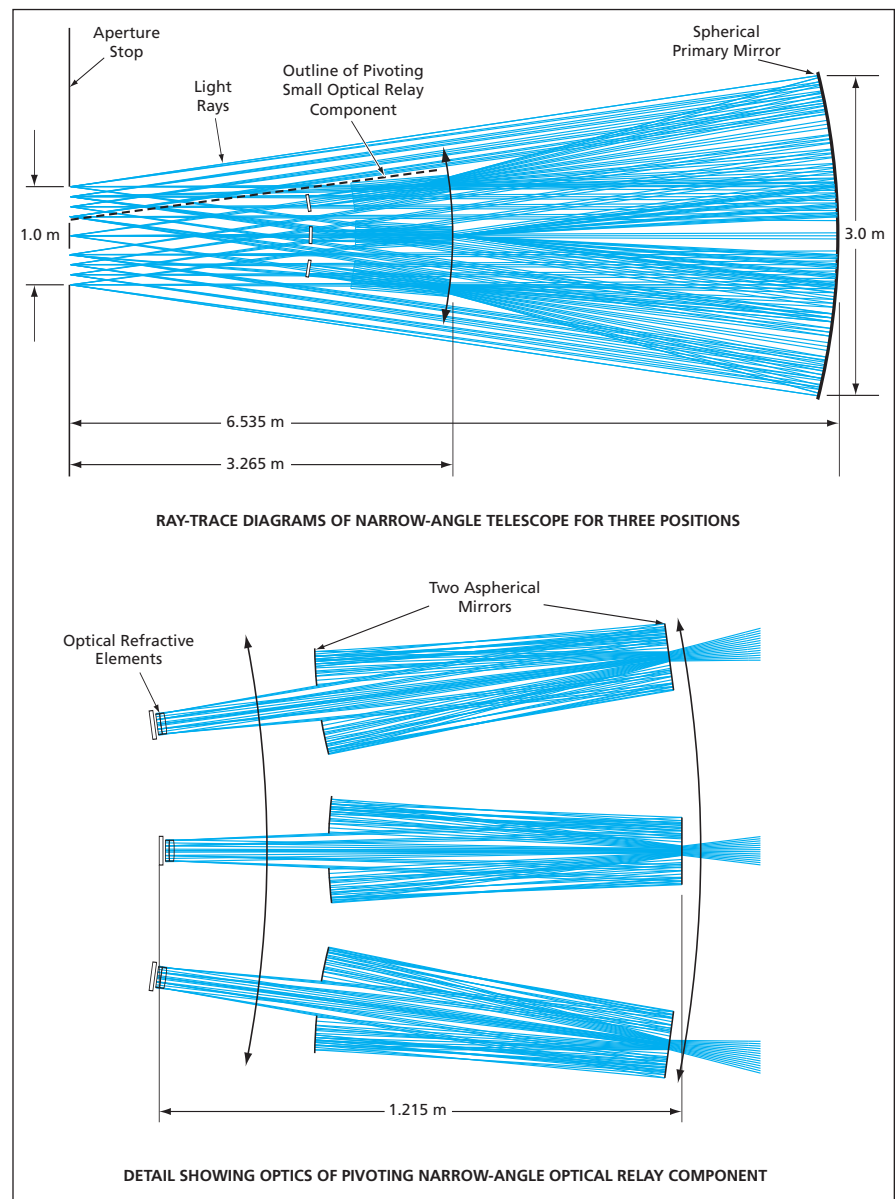
In the proposed telescope, the scanning would be effected according to a principle similar to that of the Arecibo radio telescope, in which the primary mirror is stationary with respect to the ground and a receiver is moved across the focal surface of the primary mirror. The proposed telescope would comprise (1) a large spherical primary mirror that would afford high resolution over a narrow field of view and (2) a small displaceable optical relay segment that would be pivoted about the center of an aperture stop to effect the required scanning (see figure). Taken together, both comprise a scanning narrow-angle telescope that does not require slewing the telescope structure. In normal operation, the massive telescope structure would stare at a fixed location on the ground. The inner moveable relay optic would be pivoted to scan the narrower field of view over the wider one, making it possible to retain a fixed telescope orientation, while obtaining high-resolution images over multiple target areas during an interval of 3 to 4 minutes in the intended orbit.

The pivoting relay segment of the narrow-angle telescope would include refractive and reflective optical elements, including two aspherical mirrors, to counteract the spherical aberration of the primary mirror. Overall, the combination of the pri-

mary mirror and the smaller relay optic would provide narrow-angle, diffraction-limited high resolution at a wavelength of 500 nm.

This work was done by Philip Moyni-

han, Cesar Sepulveda, Robert Wilson, and Suresh Seshadri of Caltech for NASA's Jet Propulsion Laboratory. Further information is contained in a TSP (see page 1). NPO-30891



The Design of the Spherical Primary Mirror is dictated by the requirement to cover a 16° -wide field of view without slewing the telescope. The small displaceable relay optic of the narrow-angle telescope would be pivoted about the center of the aperture stop to scan a narrower field of view (1-meter ground resolution) over the 16° field of view without the need to slew the heavier primary mirror. What is shown here is a superposition of ray-trace diagrams for the pivotable narrow-angle optical relay at its central position and two opposite extreme positions.

Multispectral Imager With Improved Filter Wheel and Optics

“Dead” time is reduced substantially, relative to prior systems of the same type.

Goddard Space Flight Center, Greenbelt, Maryland

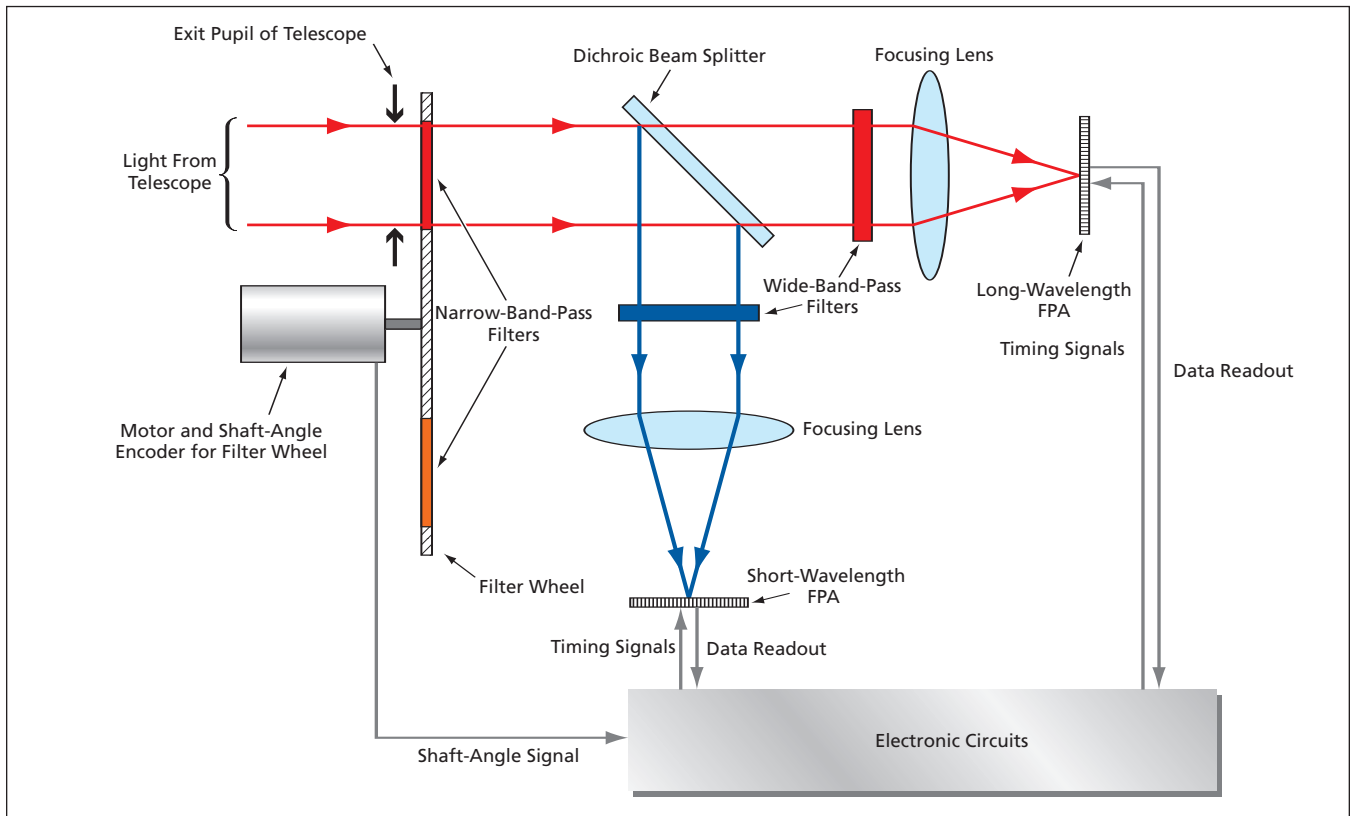


Figure 1. The Dichroic Beam Splitter and associated optics and electronics make it possible to utilize light from the telescope, even when the light beam straddles two adjacent narrow-band-pass filters. Light passed by one of these filters goes to one FPA; light passed by the other filter goes to the other FPA.

uFigure 1 schematically depicts an improved multispectral imaging system of the type that utilizes a filter wheel that contains multiple discrete narrow-band-pass filters and that is rotated at a constant high speed to acquire images in rapid succession in the corresponding spectral bands. The improvement, relative to prior systems of this type, consists of the measures taken to prevent the exposure of a focal-plane array (FPA) of photodetectors to light in more than one spectral band at any given time and to prevent exposure of the array to any light during readout. In prior systems, these measures have included, variously the use of mechanical shutters or the incorporation of wide opaque sectors (equivalent to mechanical shutters) into filter wheels. These measures introduce substantial “dead” times into each operating cycle — intervals during which image information cannot be collected and thus incoming light is

wasted. In contrast, the present improved design does not involve shutters or wide opaque sectors, and it reduces dead times substantially.

The improved multispectral imaging system is preceded by an afocal telescope and includes a filter wheel positioned so that its rotation brings each filter, in its turn, into the exit pupil of the telescope. The filter wheel contains an even number of narrow-band-pass filters separated by narrow, spokelike opaque sectors. The geometric width of each filter exceeds the cross-sectional width of the light beam coming out of the telescope. The light transmitted by the sequence of narrow-band filters is incident on a dichroic beam splitter that reflects in a broad shorter-wavelength spectral band that contains half of the narrow bands and transmits in a broad longer-wavelength spectral band that contains the other half of the narrow spectral bands. The filters are arranged on the wheel so that if the pass band of a given filter is in the re-

flexion band of the dichroic beam splitter, then the pass band of the adjacent filter is in the longer-wavelength transmission band of the dichroic beam splitter (see Figure 2).

Each of the two optical paths downstream of the dichroic beam splitter contains an additional broad-band-pass filter: The filter in the path of the light transmitted by the dichroic beam splitter transmits and attenuates in the same bands that are transmitted and reflected, respectively, by the beam splitter; the filter in the path of the light reflected by the dichroic beam splitter transmits and attenuates in the same bands that are reflected and transmitted, respectively, by the dichroic beam splitter. In each of these paths, the filtered light is focused onto an FPA.

As the filter wheel rotates at a constant angular speed, its shaft angle is monitored, and the shaft-angle signal is used to synchronize the exposure times of the two FPAs. When a single narrow-band-pass filter on the wheel occupies

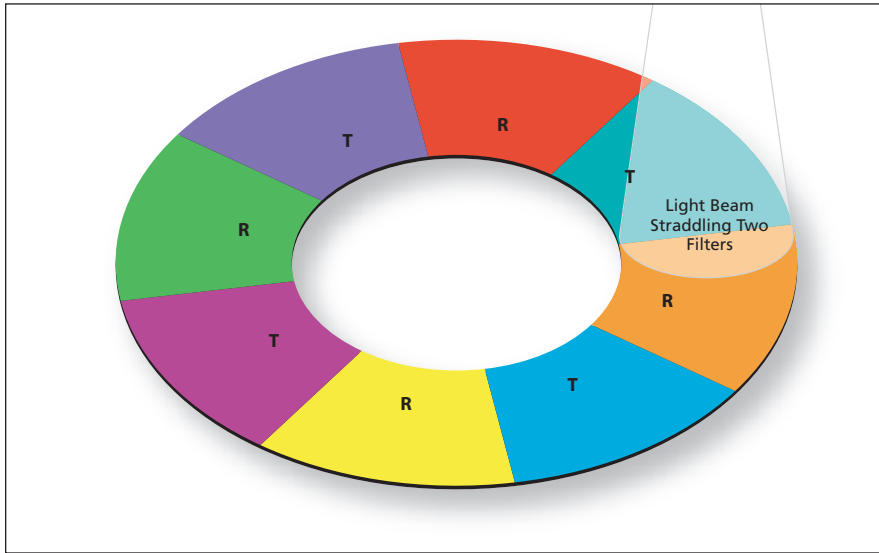


Figure 2. The **Filter Wheel** contains narrow-band-pass filters arranged so that the pass bands of adjacent filters lie, alternately, in the transmission (T) and reflection (R) spectral band of the dichroic filter.

the entire cross section of the beam of light coming out of the telescope, the spectrum of light that reaches the dichroic beam splitter lies entirely within the pass band of that filter. Therefore, the beam in its entirety is either transmitted by the dichroic beam splitter and imaged on the longer-wavelength FPA or reflected by the beam splitter and imaged onto the shorter-

wavelength FPA.

When the beam straddles two narrow-band-pass filters on the wheel, the spectrum of the light incident on the dichroic beam splitter includes one component in the transmission band and one component in the reflection band. The fraction of beam power in each component at a given instant of time is approximately equal to the frac-

tion of the cross-sectional area of the beam occupied by the corresponding narrow-band-pass filter. The out-of-band signal on each path downstream of the dichroic beam splitter is further attenuated by the broad-band-pass filter on that path. Each FPA integrates incident light during frame times synchronized with the rotation of the filter wheel. Because the dichroic filter and the broad-band-pass filter on each path block out-of-band light, each FPA can integrate a spectrally pure image, not only when the light beam is passing through a single filter, but also when it is straddling two adjacent filters.

The dichroic beam splitter and the narrow-band filters, in combination, act like a shutter for each FPA at the end of its integration period, making it possible to read out each FPA without incurring degradation of the image. The focusing lens and the FPA for each optical path downstream of the dichroic beam splitter can be optimized over a range of wavelengths spanning half the spectral bands of the system.

This work was done by James C. Bremer of Swales Aerospace for Goddard Space Flight Center. Further information is contained in a TSP (see page 1). GSC-14783-1

Integral Radiator and Storage Tank

Weight and volume are reduced.

John H. Glenn Research Center, Cleveland, Ohio

A simplified, lightweight system for dissipating heat of a regenerative fuel-cell system would include a heat pipe with its evaporator end placed at the heat source and its condenser end integrated into the wall of the regenerative fuel cell system gas-storage tanks. The tank walls act as heat-radiating surfaces for cooling the regenerative fuel cell system. The system was conceived for use in outer space, where radiation is the only physical mechanism available for transferring heat to the environment. The system could also be adapted for use on propellant tanks or other large-surface-area structures to convert them to space heat-radiating structures.

Typically for a regenerative fuel cell system, the radiator is separate from the gas-storage tanks. By using each tank's surface as a heat-radiating surface, the need for a separate, potentially massive radiator

structure is eliminated. In addition to the mass savings, overall volume is reduced because a more compact packaging scheme is possible. The underlying tank-wall structure provides ample support for heat pipes that help to distribute the heat over the entire tank surface.

The heat pipes are attached to the outer surface of each gas-storage tank by use of a high-thermal conductance, carbon-fiber composite-material wrap. Through proper choice of the composite layout, it is possible to exploit the high longitudinal conductivity of the carbon fibers (greater than the thermal conductivity of copper) to minimize the unevenness of the temperature distribution over the tank surface, thereby helping to maximize the overall heat-transfer efficiency.

In a prototype of the system, the heat-pipe and the composite wrap contribute an average mass of 340 g/m² of radiator

area. Lightweight space radiator panels have a mass of about 3,000 g/m² of radiator area, so this technique saves almost 90 percent of the mass of separate radiator panels. In tests, the modified surface of the tank was found to have an emissivity of ≈0.85. The composite wrap remained tightly bound to the surface of the tank throughout the testing in thermal vacuum conditions.

This work was done by Kenneth A Burke and John R. Miller of Glenn Research Center, and Ian Jakupca and Scott Sargi of Analex Corp. Further information is contained in a TSP (see page 1).

Inquiries concerning rights for the commercial use of this invention should be addressed to NASA Glenn Research Center, Innovative Partnerships Office, Attn: Steve Fedor, Mail Stop 4-8, 21000 Brookpark Road, Cleveland, Ohio 44135. Refer to LEW-17666-1.

Compensation for Phase Anisotropy of a Metal Reflector

A multilayer dielectric coating would introduce an opposing phase anisotropy.

NASA's Jet Propulsion Laboratory, Pasadena, California

A method of compensation for the polarization-dependent phase anisotropy of a metal reflector has been proposed. The essence of the method is to coat the reflector with multiple thin alternating layers of two dielectrics that have different indices of refraction, so as to introduce an opposing polarization-dependent phase anisotropy.

The anisotropy in question is a phenomenon that occurs in reflection of light at other than normal incidence: For a given plane wave having components polarized parallel (p) and perpendicular (s) to the plane of incidence, the

phase of s-polarized reflected light differs from the phase p-polarized light by an amount that depends on the angle of incidence and the complex index of refraction of the metal. The magnitude of the phase difference is zero at zero angle of incidence (normal incidence) and increases with the angle of incidence.

This anisotropy is analogous to a phase anisotropy that occurs in propagation of light through a uniaxial dielectric crystal. In such a case, another uniaxial crystal that has the same orientation but opposite birefringence can be used to cancel the phase

anisotropy. Although it would be difficult to prepare a birefringent material in a form suitable for application to the curved surface of a typical metal reflector in an optical instrument, it should be possible to effect the desired cancellation of phase anisotropy by exploiting the form birefringence of multiple thin dielectric layers. (The term "form birefringence" can be defined loosely as birefringence arising, in part, from a regular array of alternating subwavelength regions having different indices of refraction.)

In the proposed method, one would coat a metal reflector with alternating dielectric layers having indices of refraction n_1 and n_2 , and thicknesses d_1 and d_2 , respectively. To obtain form birefringence, the thickness of each spatial period ($d = d_1 + d_2$) must be much less than the shortest wavelength of light for which compensation is sought. For special case $d_1 = d_2 = d/2$ shown at the top of Figure 2, the resulting ordinary and extraordinary indices of refraction (n_o and n_e , respectively) would be given by

$$n_o = \left[\frac{(n_1^2 + n_2^2)}{2} \right]^{1/2}$$

and

$$n_e = n_1 n_2 \left[\frac{2}{(n_2^1 + n_2^2)} \right]^{1/2}$$

The magnitude of the compensatory phase anisotropy would be proportional to the thickness of the compensator. In choosing the thickness, one must take into account that incident light would pass through the dielectric layers, be reflected from the mirror surface, then pass through the dielectric layers again and, hence, the phase accrual through the compensation layer must therefore be doubled before being added to the reflection phase.

The free design parameters for a given application would be the choice of constituent dielectric layers (with their indices of refraction and dispersion characteristics), the thickness of the compensator (equivalently, the number of spatial periods), and the relative thickness of each constituent layer. In a typical design optimization

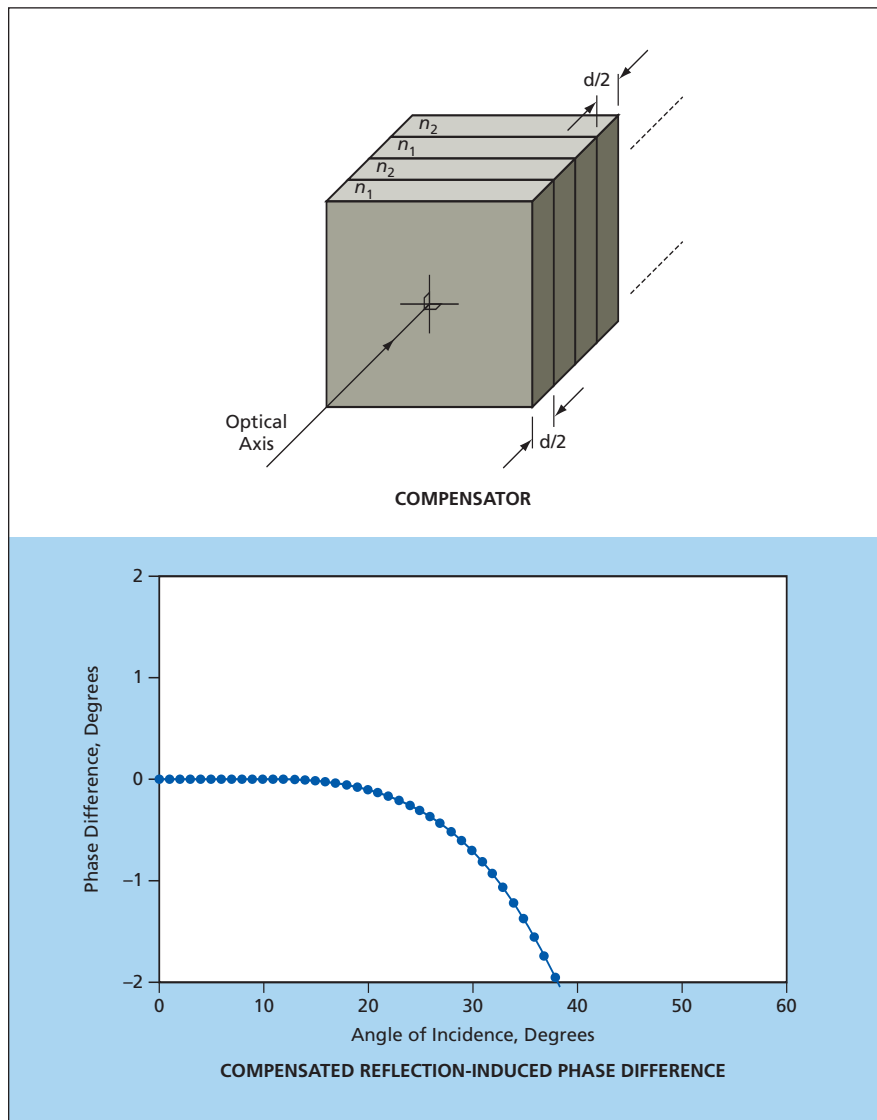


Figure 2. A Coating Comprising Alternating Thin Dielectric Layers having different indices of refraction would exhibit form birefringence that could be exploited to compensate for anisotropy like that of Figure 1.

tion, one would adapt the parameters to the reflector at hand and seek to keep the phase deviation below some maximum allowable value across the range of angles of incidence for the field of view of the instrument of which the reflector is a part. To obtain compensation over a spectral band, it would be desirable to perform a wider optimization involving the bandwidth of the

light and the dispersion characteristics of each dielectric layer.

The lower part of Figure 2 illustrates an example of compensation for the anisotropy of Figure 1 for monochromatic light. In this case a combination of $n_o = 1.5$, $n_c = 1.45$, $d_1 = d_2 = d/2$, and an overall thickness of 0.5676 wavelengths was chosen to satisfy a requirement to

keep the maximum phase anisotropy below 0.0075° at angles of incidence as large as 13° .

*This work was done by John Hong of Caltech for NASA's Jet Propulsion Laboratory. Further information is contained in a TSP (see page 1).
NPO-40728*

Optical Characterization of Molecular Contaminant Films

A theoretical model is correlated with measured spectral transmittances and VUV exposures of spacecraft optics.

Lyndon B. Johnson Space Center, Houston, Texas

A semi-empirical method of optical characterization of thin contaminant films on surfaces of optical components has been conceived. The method was originally intended for application to films that become photochemically deposited on such optical components as science windows, lenses, prisms, thin-film radiators, and glass solar-cell covers aboard spacecraft and satellites in orbit. The method should also be applicable, with suitable modifications, to thin optical films (whether deposited deliberately or formed as contaminants) on optical components used on Earth in the computer microchip laser communications and thin-film industries.

The method is expected to satisfy the need for a means of understanding and predicting the reductions in spectral transmittance caused by contaminant films and the consequent deterioration of performances of sensitive optical systems. After further development, this

method could become part of the basis of a method of designing optical systems to minimize or compensate for the deleterious effects of contaminant films. In the original outer-space application, these deleterious effects are especially pronounced because after photochemical deposition, the films become darkened by further exposure to solar vacuum ultraviolet (VUV) radiation.

In this method, thin contaminant films are theoretically modeled as thin optical films, characterized by known or assumed values of thickness, index of refraction, and absorption coefficient, that form on the outer surfaces of the original antireflection coating on affected optical components. The assumed values are adjusted as needed to make actual spectral transmittance values approximate observed ones as closely as possible and to correlate these values with amounts of VUV radiation to which the optical components have been exposed.

In an initial study, the method was applied in correlating measured changes in transmittance of high-purity fused silica photochemically coated with silicone films of various measured thicknesses and exposed to various measured amounts of VUV radiation. In each case, it was found to be possible to select an index of refraction and absorption coefficient that made the ultraviolet, visible, and infrared transmittance changes predicted by the model match the corresponding measured transmittance changes almost exactly.

This work was done by James T. Visentine of The Boeing Co. for Johnson Space Center.

This invention is owned by NASA, and a patent application has been filed. Inquiries concerning nonexclusive or exclusive license for its commercial development should be addressed to the Patent Counsel, Johnson Space Center, (281) 483-0837. Refer to MSC-23931.



Integrated Hardware and Software for No-Loss Computing

Computations on parallel processors can continue, even if one processor fails.

NASA's Jet Propulsion Laboratory, Pasadena, California

When an algorithm is distributed across multiple threads executing on many distinct processors, a loss of one of those threads or processors can potentially result in the total loss of all the incremental results up to that point. When implementation is massively hardware distributed, then the probability of a hardware failure during the course of a long execution is potentially high. Traditionally, this problem has been addressed by establishing checkpoints where the current state of some or part of the execution is saved. Then in the event of a failure, this state information can be used to recompute that point in the execution and resume the computation from that point.

A serious problem arises when one distributes a problem across multiple threads and physical processors is that one increases the likelihood of the algo-

rithm failing due to no fault of the scientist but as a result of hardware faults coupled with operating system problems. With good reason, scientists expect their computing tools to serve them and not the other way around.

What is novel here is a unique combination of hardware and software that reformulates an application into monolithic structure that can be monitored in real-time and dynamically reconfigured in the event of a failure.

This unique reformulation of hardware and software will provide advanced aeronautical technologies to meet the challenges of next-generation systems in aviation, for civilian and scientific purposes, in our atmosphere and in atmospheres of other worlds. In particular, with respect to NASA's manned flight to Mars, this technology addresses the crit-

ical requirements for improving safety and increasing reliability of manned spacecraft.

This work was done by Mark James of Caltech for NASA's Jet Propulsion Laboratory. Further information is contained in a TSP (see page 1).

In accordance with Public Law 96-517, the contractor has elected to retain title to this invention. Inquiries concerning rights for its commercial use should be addressed to:

*Innovative Technology Assets Management
JPL*

Mail Stop 202-233

4800 Oak Grove Drive

Pasadena, CA 91109-8099

(818) 354-2240

E-mail: iaoffice@jpl.nasa.gov

Refer to NPO-42554, volume and number of this NASA Tech Briefs issue, and the page number.

Decision-Tree Formulation With Order-1 Lateral Execution

Some decision trees can be transformed into objects executable by simple table lookups.

NASA's Jet Propulsion Laboratory, Pasadena, California

A compact symbolic formulation enables mapping of an arbitrarily complex decision tree of a certain type into a highly computationally efficient multidimensional software object. The type of decision trees to which this formulation applies is that known in the art as the Boolean class of balanced decision trees. Parallel lateral slices of an object created by means of this formulation can be executed in constant time — considerably less time than would otherwise be required.

Decision trees of various forms are incorporated into almost all large software systems. A decision tree is a way of hierarchically solving a problem, proceeding through a set of true/false responses to a conclusion. By definition, a decision tree has a treelike structure, wherein each internal node denotes a test on an attribute, each branch from an internal node repre-

sents an outcome of a test, and leaf nodes represent classes or class distributions that, in turn represent possible conclusions. The drawback of decision trees is that execution of them can be computationally expensive (and, hence, time-consuming) because each non-leaf node must be examined to determine whether to progress deeper into a tree structure or to examine an alternative. The present formulation was conceived as an efficient means of representing a decision tree and executing it in as little time as possible.

The formulation involves the use of a set of symbolic algorithms to transform a decision tree into a multi-dimensional object, the rank of which equals the number of lateral non-leaf nodes. The tree can then be executed in constant time by means of an order-one table lookup. The sequence of operations per-

formed by the algorithms is summarized as follows:

1. Determination of whether the tree under consideration can be encoded by means of this formulation.
2. Extraction of decision variables.
3. Symbolic optimization of the decision tree to minimize its form.
4. Expansion and transformation of all nested conjunctive-disjunctive paths to a flattened conjunctive form composed only of equality checks when possible.

If each reduced conjunctive form contains only equality checks and all of these forms use the same variables, then the decision tree can be reduced to an order-one operation through a table lookup. The speedup to order one is accomplished by distributing each decision variable over a surface of a multidimensional object by mapping the equality constant to an index.

The disadvantage of this formulation is that it requires mapping of each equality constant to a small range in order to keep the multidimensional object small. However, if each constant is reduced to a small range through preprocessing,

then the result will be optimal in both time and space.

*This work was done by Mark James of Caltech for **NASA's Jet Propulsion Laboratory**. Further information is contained in a TSP (see page 1).*

The software used in this innovation is available for commercial licensing. Please contact Karina Edmonds of the California Institute of Technology at (626) 395-2322. Refer to NPO-42004.



GIS Methodology for Planning Planetary-Rover Operations

A document describes a methodology for utilizing image data downlinked from cameras aboard a robotic ground vehicle (rover) on a remote planet for analyzing and planning operations of the vehicle and of any associated spacecraft. Traditionally, the cataloging and presentation of large numbers of downlinked planetary-exploration images have been done by use of two organizational methods: temporal organization and correlation between activity plans and images. In contrast, the present methodology involves spatial indexing of image data by use of the computational discipline of geographic information systems (GIS), which has been maturing in terrestrial applications for decades, but, until now, has not been widely used in support of exploration of remote planets. The use of GIS to catalog data products for analysis is intended to increase efficiency and effectiveness in planning rover operations, just as GIS has proven to be a source of powerful computational tools in such terrestrial endeavors as law enforcement, military strategic planning, surveying, political science, and epidemiology. The use of GIS also satisfies the need for a map-based user interface that is intuitive to rover-activity planners, many of whom are deeply familiar with maps and know how to use them effectively in field geology.

This work was done by Mark Powell, Jeffrey Norris, Jason Fox, Kenneth Rabe, and I-Hsiang Shu of Caltech for NASA's Jet Propulsion Laboratory. Further information is contained in a TSP (see page 1).

This software is available for commercial licensing. Please contact Karina Edmonds of the California Institute of Technology at (626) 395-2322. Refer to NPO-41812.

Optimal Calibration of the Spitzer Space Telescope

A document discusses the focal-plane calibration of the Spitzer Space Telescope by use of the instrument pointing frame (IPF) Kalman filter, which was described in "Kalman Filter for Calibrating a Telescope Focal Plane" (NPO-40798),

NASA Tech Briefs, Vol. 30, No. 9 (September 2006), page 62. To recapitulate: In the IPF Kalman filter, optimal estimates of both engineering and scientific focal-plane parameters are obtained simultaneously, using data taken in each focal-plane survey activity. The IPF Kalman filter offers greater efficiency and economy, relative to prior calibration practice in which scientific and engineering parameters were estimated by separate teams of scientists and engineers and iterated upon each other. In the Spitzer Space Telescope application, the IPF Kalman filter was used to calibrate 56 frames for precise telescope pointing, estimate >1,500 parameters associated with focal-plane mapping, and process calibration runs involving as many as 1,338 scientific image centroids. The final typical survey calibration accuracy was found to be 0.09 arc second. The use of the IPF Kalman filter enabled a team of only four analysts to complete the calibration processing in three months. An unanticipated benefit afforded by the IPF Kalman filter was the ability to monitor health and diagnose performance of the entire end-to-end telescope-pointing system.

This work was done by David Bayard, Bryan Kang, Paul Brugarolas, and Dhemetrio Boussalis of Caltech for NASA's Jet Propulsion Laboratory. Further information is contained in a TSP (see page 1).

The software used in this innovation is available for commercial licensing. Please contact Karina Edmonds of the California Institute of Technology at (626) 395-2322. Refer to NPO-41178.

Automated Detection of Events of Scientific Interest

A report presents a slightly different perspective of the subject matter of "Fusing Symbolic and Numerical Diagnostic Computations" (NPO-42512), which appears elsewhere in this issue of NASA Tech Briefs. Briefly, the subject matter is the X-2000 Anomaly Detection Language, which is a developmental computing language for fusing two diagnostic computer programs — one implementing a numerical analysis method, the other implementing a symbolic analysis method — into a unified event-based decision analysis software

system for real-time detection of events. In the case of the cited companion NASA Tech Briefs article, the contemplated events that one seeks to detect would be primarily failures or other changes that could adversely affect the safety or success of a spacecraft mission. In the case of the instant report, the events to be detected could also include natural phenomena that could be of scientific interest. Hence, the use of X-2000 Anomaly Detection Language could contribute to a capability for automated, coordinated use of multiple sensors and sensor-output-data-processing hardware and software to effect opportunistic collection and analysis of scientific data.

This work was done by Mark James of Caltech for NASA's Jet Propulsion Laboratory. Further information is contained in a TSP (see page 1).

In accordance with Public Law 96-517, the contractor has elected to retain title to this invention. Inquiries concerning rights for its commercial use should be addressed to:

Innovative Technology Assets Management

JPL

Mail Stop 202-233

4800 Oak Grove Drive

Pasadena, CA 91109-8099

(818) 354-2240

E-mail: iaoffice@jpl.nasa.gov

Refer to NPO-42513, volume and number of this NASA Tech Briefs issue, and the page number.

Representation-Independent Iteration of Sparse Data Arrays

An approach is defined that describes a method of iterating over massively large arrays containing sparse data using an approach that is implementation independent of how the contents of the sparse arrays are laid out in memory. What is unique and important here is the decoupling of the iteration over the sparse set of array elements from how they are internally represented in memory. This enables this approach to be backward compatible with existing schemes for representing sparse arrays as well as new approaches. What is novel here is a new approach for efficiently iterating over

sparse arrays that is independent of the underlying memory layout representation of the array. A functional interface is defined for implementing sparse arrays in any modern programming language with a particular focus for the Chapel programming language. Examples are provided that show the translation of a loop that computes a matrix vector product into this representation for both the distributed and not-distributed cases. This work is directly applicable to NASA and its High Productivity Computing Systems (HPCS) program that JPL and our current program are engaged in. The goal of this program is to create powerful, scalable, and economically viable high-powered computer systems suitable for use in national security and industry by 2010. This is important to NASA for its computationally intensive requirements for analyzing and understanding the volumes of science data from our returned missions.

This work was done by Mark James of Caltech for NASA's Jet Propulsion Laboratory. Further information is contained in a TSP (see page 1).

The software used in this innovation is available for commercial licensing. Please contact Karina Edmonds of the California Institute of Technology at (626) 395-2322. Refer to NPO-42502.

Mission Operations of the Mars Exploration Rovers

A document describes a system of processes involved in planning, com-

manding, and monitoring operations of the rovers Spirit and Opportunity of the Mars Exploration Rover mission. The system is designed to minimize command turnaround time, given that inherent uncertainties in terrain conditions and in successful completion of planned landed spacecraft motions preclude planning of some spacecraft activities until the results of prior activities are known by the ground-based operations team. The processes are partitioned into those (designated as tactical) that must be tied to the Martian clock and those (designated strategic) that can, without loss, be completed in a more leisurely fashion. The tactical processes include assessment of downlinked data, refinement and validation of activity plans, sequencing of commands, and integration and validation of sequences. Strategic processes include communications planning and generation of long-term activity plans. The primary benefit of this partition is to enable the tactical portion of the team to focus solely on tasks that contribute directly to meeting the deadlines for commanding the rover's each sol (1 sol = 1 Martian day) — achieving a turnaround time of 18 hours or less, while facilitating strategic team interactions with other organizations that do not work on a Mars time schedule.

This work was done by Deborah Bass, Sharon Lauback, Andrew Mishkin, and Daniel Limonadi of Caltech for NASA's Jet Propulsion Laboratory. Further information is contained in a TSP (see page 1).

The software used in this innovation is available for commercial licensing. Please contact Karina Edmonds of the California

Institute of Technology at (626) 395-2322. Refer to NPO-42471.

More About Software for No-Loss Computing

A document presents some additional information on the subject matter of "Integrated Hardware and Software for No-Loss Computing" (NPO-42554), which appears elsewhere in this issue of *NASA Tech Briefs*. To recapitulate: The hardware and software designs of a developmental parallel computing system are integrated to effectuate a concept of no-loss computing (NLC). The system is designed to reconfigure an application program such that it can be monitored in real time and further reconfigured to continue a computation in the event of failure of one of the computers. The design provides for (1) a distributed class of NLC computation agents, denoted introspection agents, that effects hierarchical detection of anomalies; (2) enhancement of the compiler of the parallel computing system to cause generation of state vectors that can be used to continue a computation in the event of a failure; and (3) activation of a recovery component when an anomaly is detected.

This work was done by Mark James of Caltech for NASA's Jet Propulsion Laboratory. Further information is contained in a TSP (see page 1).

The software used in this innovation is available for commercial licensing. Please contact Karina Edmonds of the California Institute of Technology at (626) 395-2322. Refer to NPO-42511



National Aeronautics and
Space Administration